

# Regression-Based Single-Point Zeroth-Order Optimization

Xin Chen<sup>†\*</sup>

Department of Electrical and Computer Engineering  
Texas A&M University  
xin\_chen@tamu.edu

Zhaolin Ren<sup>†</sup>

School of Engineering and Applied Science  
Harvard University  
zhaolinren@g.harvard.edu

## Abstract

Zeroth-order optimization (ZO) is widely used for solving black-box optimization and control problems. In particular, single-point ZO (SZO) is well-suited to online or dynamic problem settings due to its requirement of only a single function evaluation per iteration. However, SZO suffers from high gradient estimation variance and slow convergence, which severely limit its practical applicability. Despite recent advances, the convergence of existing SZO methods remains inferior to that of two-point ZO methods. To overcome this limitation, we propose a novel yet simple SZO framework, termed regression-based SZO (RESZO), which substantially enhances the convergence rate. Unlike conventional ZO methods that rely solely on function evaluations at the current point for gradient estimation, RESZO improves gradient estimation by effectively leveraging historical function evaluations from previous iterations. Specifically, RESZO constructs a surrogate function via regression using recent historical evaluations and employs the gradient of this surrogate function for iterative updates. Two variants of RESZO, which fit linear and quadratic surrogate functions respectively, are introduced. Theoretically, we provide a non-asymptotic convergence analysis for the linear variant of RESZO, showing that its convergence rates are comparable to those of two-point ZO methods for both smooth nonconvex and strongly convex functions. Moreover, extensive numerical experiments demonstrate that RESZO not only matches but empirically outperforms two-point ZO in terms of function query complexity.

## 1 Introduction

In this paper, we consider solving a generic black-box unconstrained optimization problem (1):

$$\min_{\mathbf{x} \in \mathbb{R}^d} f(\mathbf{x}), \quad (1)$$

where  $\mathbf{x} \in \mathbb{R}^d$  is the decision variable of dimension  $d$ . The objective function  $f : \mathbb{R}^d \rightarrow \mathbb{R}$  is unknown, and only its zeroth-order information, namely function evaluations, is accessible. As a result, the first-order gradients of function  $f$  are unavailable, and problem (1) can be solved solely based on function evaluations. This type of black-box optimization problems has attracted considerable

---

\*Corresponding author.

<sup>†</sup>X. Chen and Z. Ren contributed equally to this work.

recent attention and covers a broad range of applications, including power system control [1, 2], reinforcement learning [3, 4], neural network training [5, 6], sensor management [7], etc.

Zeroth-order optimization (ZO) methods [7, 8] have been extensively developed and applied to solve black-box optimization problems, offering theoretical convergence guarantees. Essentially, ZO methods estimate unknown gradients using perturbed function evaluations. According to the number of queried function evaluations per iteration, ZO methods can be categorized into single-point, two-point, and multi-point ZO schemes [7]. Single-point ZO (SZO) methods [9, 10, 11] require only a single function evaluation per iteration for gradient estimation, making them well-suited for online optimization or dynamic control applications. Because in such settings, the system environment is non-stationary, or each function evaluation involves implementing a decision that directly changes the system environment, rendering multiple function queries at the same instant infeasible. However, single-point ZO suffers from large estimation variance and slow convergence, severely limiting its practical applicability. Despite recent advancements [10, 11, 12, 13, 14], the convergence of single-point ZO remains slower than that of two-point ZO or multi-point ZO, which use multiple function evaluations for gradient estimation per iteration and achieve lower variance.

**Motivation.** At each iteration  $t$ , classic ZO methods estimate the gradient  $\nabla f(\mathbf{x}_t)$  solely based on the function evaluations at the current point  $\mathbf{x}_t$ , while all historical function evaluations obtained from previous iterations are discarded. However, these past function evaluations contain valuable information about the unknown function and can help with the gradient estimations for subsequent iterations, especially those obtained in the most recent iterations. Moreover, in many practical applications, such as clinical trials, real-world experiments, and long-term complex simulations, obtaining a single function evaluation can be costly and laborious, making it crucial to fully exploit all available evaluations to enhance efficiency. Then, a natural question is

*“Can available historical function evaluations from previous iterations be leveraged to enhance single-point zeroth-order gradient estimation?”*

**Contribution.** Motivated by this question, we propose a novel yet simple single-point ZO framework, termed **Regression-based Single-point Zeroth-order Optimization (RESZO)**. In contrast to classic ZO methods that rely solely on function evaluations at the current point for gradient estimation, the proposed RESZO method significantly enhances gradient estimation by leveraging available historical function evaluations from previous iterations. Specifically, the RESZO method queries the function value only once at each iteration, and fits a surrogate model based on recent historical function evaluations via regression. Then, the surrogate model’s gradient is used as the estimated gradient for iterative updates. We introduce two variants of the RESZO method, termed L-RESZO and Q-RESZO, which fit linear and quadratic surrogate functions, respectively. A key ingredient of the proposed RESZO method is adding random perturbations to function evaluations to ensure sufficient exploration. Theoretically (see Table 1), we show that for both smooth nonconvex and strongly convex functions, the linear variant of our algorithm (L-RESZO) achieves convergence rates that are only worse than those of two-point ZO methods by a factor  $C_d > 0$ , where  $C_d$  is a parameter defined in (21) in Assumption 2. This represents a substantial improvement over the rates achieved by existing SZO methods (see Table 1). While theoretically bounding the term  $C_d$  is challenging, strong empirical evidence shows that  $C_d$  scales as  $\mathcal{O}(\sqrt{d})$  under appropriate algorithmic settings; see Section 4 for more details. To the best of our knowledge, this is the first work to present single-point ZO methods whose convergence rates match those of two-point ZO methods. Moreover, extensive numerical experiments demonstrate that RESZO not only matches but empirically *outperforms* two-point ZO in terms of function query complexity.

**Related Work.** The classic SZO method, formulated in (2), is first proposed by [9], which

Table 1: Iteration complexity of ZO methods for solving Lipschitz and smooth objective functions.

Method	Literature	Complexity	
		$\mu$ -Strongly convex	Non-convex
Classic SZO	[14]	$\mathcal{O}(d^2/\varepsilon^3)$	–
Residual-feedback SZO	[15]	$\mathcal{O}(d^3/\varepsilon^{\frac{3}{2}})$	$\mathcal{O}(d^3/\varepsilon^{\frac{3}{2}})$
HLF-SZO	[11]	$\mathcal{O}(d^{\frac{3}{2}}/\varepsilon^{\frac{3}{2}})$	$\mathcal{O}(d^{\frac{3}{2}}/\varepsilon^{\frac{3}{2}})$
<b>L-RESZO</b>	<b>THIS WORK</b>	$\mathcal{O}(C_d \frac{d}{\mu} \log \frac{1}{\varepsilon})$	$\mathcal{O}(C_d d/\varepsilon)$
Two-point ZO	[8]	$\mathcal{O}(\frac{d}{\mu} \log \frac{1}{\varepsilon})$	$\mathcal{O}(d/\varepsilon)$

\*In the strongly convex case, the accuracy is measured by  $f(x_T) - f^* \leq \varepsilon$ , where  $f^* := \min_{x \in \mathbb{R}^d} f(x)$ . In the non-convex case, the accuracy is measured by  $\frac{1}{T} \sum_{k=1}^T \|\nabla f(x_k)\|^2 \leq \varepsilon$ .

estimates gradients by querying only a single function value per iteration. In [13], a self-concordant barrier function is used to enhance the convergence of SZO for solving bandit smooth convex optimization. By leveraging high-order smoothness, reference [16] derives an improved complexity bound for SZO in the context of stochastic convex optimization. To further enhance the convergence of SZO, reference [15] proposes a residual-feedback SZO method, formulated in (3), which reuses the function evaluation from the last iteration for gradient estimation, resulting in significant performance improvement. Additionally, reference [11] leverages the idea of high-pass and low-pass filters from extremum seeking control to accelerate SZO convergence. Notably, the integration of a high-pass filter coincides with the residual-feedback approach in [15]. This paper follows a similar direction to [11, 15]; however, rather than reusing only the most recent function evaluation, we leverage many historical function evaluations from previous iterations to fit surrogate models. In addition, our RESZO method is related to the linear regression and interpolation approaches [17, 18, 19] used in derive-free optimization (DFO) [20]. The fundamental difference is that these methods [17, 18, 19] perform multiple function evaluations near the current point for linear interpolation or regression. In contrast, our approach queries the function value only once at each iteration and fits surrogate models by fully recycling historical function evaluations from past iterations.

## 2 Preliminaries on Zeroth-Order Optimization

The classic single-point ZO (SZO) method [9] that solves (1) is given by (2):

$$\text{Single-point ZO (SZO)} : \mathbf{x}_{t+1} = \mathbf{x}_t - \eta \cdot \underbrace{\frac{d}{\delta} f(\mathbf{x}_t + \delta \mathbf{u}_t) \mathbf{u}_t}_{:= \mathbf{G}_f^1(\mathbf{x}_t; \mathbf{u}_t, \delta)}, \quad t = 0, 1, 2, \dots \quad (2)$$

where  $\delta > 0$  is a scalar parameter called smoothing radius,  $\eta > 0$  is the step size, and  $\mathbf{u}_t \in \mathbb{R}^d$  is an independent identically distributed random direction vector sampled from  $\text{Unif}(\mathbb{S}_{d-1})$ , namely the uniform distribution on the unit sphere  $\mathbb{S}_{d-1}$ , for all  $k = 0, 1, 2, \dots$ . The random direction vector  $\mathbf{u}_t$  can also be sampled from the multivariate Gaussian distribution  $\mathcal{N}(\mathbf{0}, \mathbf{I})$  or other zero-mean distributions. In (2),  $\mathbf{G}_f^1(\mathbf{x}_t; \mathbf{u}_t, \delta)$  denotes the SZO gradient estimator of function  $f$ .

Recent works [15, 11] have introduced a new variant of SZO, referred to as residual-feedback SZO (RSZO) [15] or high-pass filter-integrated SZO [11], which is given by (3):

**Residual-feedback SZO (RSZO) :**

$$\mathbf{x}_{t+1} = \mathbf{x}_t - \eta \cdot \underbrace{\frac{d}{\delta} \left( f(\mathbf{x}_t + \delta \mathbf{u}_t) - f(\mathbf{x}_{t-1} + \delta \mathbf{u}_{t-1}) \right)}_{:= \mathbf{G}_f^1(\mathbf{x}_t; \mathbf{u}_t, \delta)} \mathbf{u}_t, \quad t = 1, 2, \dots \quad (3)$$

At each iteration  $t$ , the gradient estimator  $\mathbf{G}_f^1(\mathbf{x}_t; \mathbf{u}_t, \delta)$  of the RSZO method (3) reuses the function evaluation  $f(\mathbf{x}_{t-1} + r\mathbf{u}_{t-1})$  queried at the last iteration  $t-1$ . This approach substantially reduces gradient estimation variance and improves convergence compared with SZO (2).

The classic two-point ZO (TZO) method [8] that solves problem (1) is given by (4):

**Two-point ZO (TZO) :**

$$\mathbf{x}_{t+1} = \mathbf{x}_t - \eta \cdot \underbrace{\frac{d}{2\delta} \left( f(\mathbf{x}_t + \delta \mathbf{u}_t) - f(\mathbf{x}_t - \delta \mathbf{u}_t) \right)}_{:= \mathbf{G}_f^2(\mathbf{x}_t; \mathbf{u}_t, \delta)} \mathbf{u}_t, \quad t = 0, 1, 2, \dots, \quad (4)$$

which employs two function evaluations to estimate the gradient of function  $f$  with the two-point gradient estimator  $\mathbf{G}_f^2(\mathbf{x}_t; \mathbf{u}_t, \delta)$ .

The classic ZO gradient estimators above share the same expectation [8]:

$$\begin{aligned} \mathbb{E}_{\mathbf{u} \sim \text{Unif}(\mathbb{S}_{d-1})} [\mathbf{G}_f^1(\mathbf{x}; \mathbf{u}, \delta)] &= \mathbb{E}_{\mathbf{u} \sim \text{Unif}(\mathbb{S}_{d-1})} [\mathbf{G}_f^1(\mathbf{x}; \mathbf{u}, \delta)] \\ &= \mathbb{E}_{\mathbf{u} \sim \text{Unif}(\mathbb{S}_{d-1})} [\mathbf{G}_f^2(\mathbf{x}; \mathbf{u}, \delta)] = \nabla \hat{f}(\mathbf{x}; \delta), \end{aligned} \quad (5)$$

where  $\hat{f}(\mathbf{x}; \delta) := \mathbb{E}_{\mathbf{v} \sim \text{Unif}(\mathbb{B}_d)} [f(\mathbf{x} + \delta \mathbf{v})]$  is a smoothed version of the original function  $f$  [9]. Despite having the same expectation, the two-point ZO gradient estimator  $\mathbf{G}_f^2(\mathbf{x}_t; \mathbf{u}_t, \delta)$  exhibits lower variance and achieves faster convergence, compared with the single-point ZO gradient estimators  $\mathbf{G}_f^1(\mathbf{x}_t; \mathbf{u}_t, \delta)$  and  $\mathbf{G}_f^1(\mathbf{x}_t; \mathbf{u}_t, \delta)$ . See [8, 11] for more details.

### 3 Regression-Based Single-Point Zeroth-Order Optimization

In this paper, we focus on the class of SZO methods that require only one function evaluation per iteration. Below, we introduce the proposed RESZO method and two specific variants, L-RESZO and Q-RESZO, which fit linear and quadratic surrogate models using historical function evaluations.

#### 3.1 Linear Regression-Based Single-Point Zeroth-Order Optimization (L-RESZO)

At each iteration  $t$ , the available function evaluations from all previous iterations are given by  $\{f(\hat{\mathbf{x}}_k)\}_{k=0}^t$  with  $\hat{\mathbf{x}}_k = \mathbf{x}_k + \delta \mathbf{u}_k$ . Here,  $\mathbf{u}_k \in \mathbb{R}^d$  is a random direction vector sampled from the uniform distribution  $\text{Unif}(\mathbb{S}_{d-1})$  over the unit sphere  $\mathbb{S}_{d-1}$ , or from the multivariate Gaussian distribution  $\mathcal{N}(\mathbf{0}, \mathbf{I})$ ; and  $\delta > 0$  is a scalar parameter called smoothing radius. These are consistent with the classic ZO methods (2)-(4). Note that function evaluations are performed at the perturbed points  $\hat{\mathbf{x}}_k$  rather than the iterate points  $\mathbf{x}_k$  to promote sufficient exploration of the optimization space. The necessity of introducing such perturbations is further illustrated by Remark 1 and the numerical experiments in Section 5.2.

Based on the first-order Taylor expansion at the current perturbed point  $\hat{\mathbf{x}}_t$ , the available function evaluations  $\{f(\hat{\mathbf{x}}_k)\}_{k=0}^t$  can be expressed as (6):

$$f(\hat{\mathbf{x}}_k) = f(\hat{\mathbf{x}}_t) + \nabla f(\hat{\mathbf{x}}_t)^\top (\hat{\mathbf{x}}_k - \hat{\mathbf{x}}_t) + \epsilon_{t,k}, \quad k = 0, 1, \dots, t, \quad (6)$$

where  $\epsilon_{t,k}$  denotes the corresponding high-order residual term. Accordingly, we propose to fit a linear surrogate function  $f_t^{\text{sl}}(\mathbf{x})$  in (7) to locally approximate the original function  $f(\mathbf{x})$  in (1):

$$f_t^{\text{sl}}(\mathbf{x}) := f(\hat{\mathbf{x}}_t) + \mathbf{g}_t^\top (\mathbf{x} - \hat{\mathbf{x}}_t) + c_t, \quad (7)$$

where the linear coefficient vector  $\mathbf{g}_t \in \mathbb{R}^d$  and the intercept  $c_t \in \mathbb{R}$  can be obtained through linear regression on the available sample points  $\{\hat{\mathbf{x}}_k, f(\hat{\mathbf{x}}_k)\}_{k=0}^t$ . Then, the gradient of the surrogate function  $\nabla f_t^{\text{sl}}(\mathbf{x}) = \mathbf{g}_t$  can be used as the estimator for the true gradient  $\nabla f(\mathbf{x})$ .

To ensure that the fitted surrogate model  $f_t^{\text{sl}}(\mathbf{x})$  remains up-to-date with the most recent function evaluations, we employ the recursive linear regression in a sliding window, which uses only the latest  $m$  function evaluations  $\{\hat{\mathbf{x}}_{t-i+1}, f(\hat{\mathbf{x}}_{t-i+1})\}_{i=1}^m$  to fit the linear model at each iteration  $t$ . Specifically, at each iteration  $t$ , we solve the following least squares problem (8) to obtain  $\mathbf{g}_t$  and  $c_t$ :

$$\min_{\mathbf{g}_t, c_t} \sum_{i=1}^m \left[ f_t^{\text{sl}}(\hat{\mathbf{x}}_{t-i+1}) - f(\hat{\mathbf{x}}_{t-i+1}) \right]^2 \implies \begin{bmatrix} \mathbf{g}_t \\ c_t \end{bmatrix} = (X_t^\top X_t)^\dagger X_t^\top \mathbf{y}_t, \quad (8)$$

where  $\dagger$  denotes the Moore–Penrose pseudoinverse,  $\Delta_{t,i}^x := \hat{\mathbf{x}}_{t-i+1} - \hat{\mathbf{x}}_t$ ,  $\Delta_{t,i}^f := f(\hat{\mathbf{x}}_{t-i+1}) - f(\hat{\mathbf{x}}_t)$ ,

$$X_t := \begin{bmatrix} \Delta_{t,1}^x \top & 1 \\ \Delta_{t,2}^x \top & 1 \\ \vdots & \vdots \\ \Delta_{t,m}^x \top & 1 \end{bmatrix} \in \mathbb{R}^{m \times (d+1)}, \quad \mathbf{y}_t := \begin{bmatrix} \Delta_{t,1}^f \\ \Delta_{t,2}^f \\ \vdots \\ \Delta_{t,m}^f \end{bmatrix} \in \mathbb{R}^m. \quad (9)$$

Consequently, the proposed **Linear Regression-based Single-point Zeroth-order Optimization (L-RESZO)** method for solving problem (1) is presented as Algorithm 1. Since the linear regression requires  $m$  function evaluations, we initially employ a classical ZO algorithm, such as the RSZO method (3), to perform iterative updates and accumulate sufficient sample points, as shown in Step 3. After  $m$  iterations, the algorithm switches to using the linear regression-based gradient estimator  $\mathbf{g}_t$  for subsequent iterative updates, as shown in Steps 6–8.

---

**Algorithm 1: Linear Regression-based Single-point Zeroth-order Optimization (L-RESZO)**

---

- 1: **Inputs:** Initial point  $\mathbf{x}_0$ , stepsizes  $\tilde{\eta}, \eta$ , smoothing radius values  $\tilde{\delta}, \delta$ , sample size  $m$ , and total iteration number  $T$ .
  - 2: **for**  $t = 0 : m - 1$  **do**
  - 3:   Perform the RSZO method (3) with  $\tilde{\eta}, \tilde{\delta}$  for iterative updates.
  - 4: **end for**
  - 5: **for**  $t = m : T$  **do**
  - 6:   Randomly sample  $\mathbf{u}_t \sim \text{Unif}(\mathbb{S}_{d-1})$ ; perform a function evaluation on the perturbed value  $\hat{\mathbf{x}}_t = \mathbf{x}_t + \delta \mathbf{u}_t$  to obtain  $f(\hat{\mathbf{x}}_t)$ ; collect  $m$  latest sample points  $\{\hat{\mathbf{x}}_{t-i+1}, f(\hat{\mathbf{x}}_{t-i+1})\}_{i=1}^m$ .
  - 7:   Solve for the linear coefficient  $\mathbf{g}_t$  via (8).
  - 8:   Update with  $\mathbf{x}_{t+1} = \mathbf{x}_t - \eta \cdot \mathbf{g}_t$ .
  - 9: **end for**
- 

In addition, the sample size  $m$  is typically chosen to be comparable to the dimension  $d$  of  $\mathbf{x}$ , or slightly larger, to ensure that  $X_t$  is of full column rank and the matrix  $X_t^\top X_t$  in (8) is invertible. In this case, one can replace the pseudoinverse  $(\cdot)^\dagger$  in (8) by the regular matrix inverse  $(\cdot)^{-1}$ .

**Fast Computation of Matrix Inverse.** When the matrix  $X_t^\top X_t$  in (8) is invertible, the rank-1 update approach [21] can be employed to enable fast computation of the matrix inverse.

Note that performing linear regression based on the sample point set  $\{\Delta_{t,i}^x, \Delta_{t,i}^f\}_{i=1}^m$  yields the same linear coefficient  $\mathbf{g}_t$  as linear regression on the sample point set  $\{\hat{\mathbf{x}}_{t-i+1}, f(\hat{\mathbf{x}}_{t-i+1})\}_{i=1}^m$ . This equivalence holds because the former set is simply a translational shift of the latter by  $(\hat{\mathbf{x}}_t, f(\hat{\mathbf{x}}_t))$  in the coordinate space. Hence, the least squares problem (8) based on  $\{\Delta_{t,i}^x, \Delta_{t,i}^f\}_{i=1}^m$  can be replaced by the least squares problem (10) based on  $\{\hat{\mathbf{x}}_{t-i+1}, f(\hat{\mathbf{x}}_{t-i+1})\}_{i=1}^m$  to obtain  $\mathbf{g}_t$ :

$$\min_{\mathbf{g}_t, c_t} \sum_{i=1}^m \left( \mathbf{g}_t^\top \hat{\mathbf{x}}_{t-i+1} + c_t - f(\hat{\mathbf{x}}_{t-i+1}) \right)^2 \implies \begin{bmatrix} \mathbf{g}_t \\ c_t \end{bmatrix} = (\hat{X}_t^\top \hat{X}_t)^{-1} \hat{X}_t^\top \hat{\mathbf{y}}_t, \quad (10)$$

where

$$\hat{X}_t := \begin{bmatrix} \hat{\mathbf{x}}_t^\top & 1 \\ \hat{\mathbf{x}}_{t-1}^\top & 1 \\ \vdots & \vdots \\ \hat{\mathbf{x}}_{t-m+1}^\top & 1 \end{bmatrix} \in \mathbb{R}^{m \times (d+1)}, \quad \hat{\mathbf{y}}_t := \begin{bmatrix} f(\hat{\mathbf{x}}_t) \\ f(\hat{\mathbf{x}}_{t-1}) \\ \vdots \\ f(\hat{\mathbf{x}}_{t-m+1}) \end{bmatrix} \in \mathbb{R}^m. \quad (11)$$

Consequently, when moving from iteration  $t$  to  $t+1$ , the matrix  $\hat{X}_{t+1}$  is actually formed by dropping the oldest sample point  $\hat{\mathbf{x}}_{t-m+1}$  from  $\hat{X}_t$  and adding the latest sample point  $\hat{\mathbf{x}}_{t+1}$  to it. This leads to the update rule (12):

$$\hat{X}_{t+1}^\top \hat{X}_{t+1} = \hat{X}_t^\top \hat{X}_t - \hat{\mathbf{x}}_{t-m+1} \hat{\mathbf{x}}_{t-m+1}^\top + \hat{\mathbf{x}}_{t+1} \hat{\mathbf{x}}_{t+1}^\top. \quad (12)$$

Hence, given the available matrix inverse  $(\hat{X}_t^\top \hat{X}_t)^{-1}$  obtained in the last iteration, the new matrix inverse  $(\hat{X}_{t+1}^\top \hat{X}_{t+1})^{-1}$  can be computed efficiently as (13) by using the Sherman–Morrison–Woodbury formula [21] twice in a row: one for dropping  $\hat{\mathbf{x}}_{t-m+1}$  and the other for adding  $\hat{\mathbf{x}}_{t+1}$ ;

$$B = A + \frac{A \hat{\mathbf{x}}_{t-m+1} \hat{\mathbf{x}}_{t-m+1}^\top A}{1 - \hat{\mathbf{x}}_{t-m+1}^\top A \hat{\mathbf{x}}_{t-m+1}}, \quad (\hat{X}_{t+1}^\top \hat{X}_{t+1})^{-1} = B - \frac{B \hat{\mathbf{x}}_{t+1} \hat{\mathbf{x}}_{t+1}^\top B}{1 + \hat{\mathbf{x}}_{t+1}^\top B \hat{\mathbf{x}}_{t+1}}, \quad (13)$$

where  $A := (\hat{X}_t^\top \hat{X}_t)^{-1}$  and  $B := (\hat{X}_t^\top \hat{X}_t - \hat{\mathbf{x}}_{t-m+1} \hat{\mathbf{x}}_{t-m+1}^\top)^{-1}$ .

This approach avoids recomputing the new matrix inverse  $(\hat{X}_{t+1}^\top \hat{X}_{t+1})^{-1}$  from scratch and reduces the computational cost of matrix inversion from  $\mathcal{O}(d^3)$  to  $\mathcal{O}(d^2)$ .

*Remark 1. (Role of Perturbation).* From (11), it is seen that the rows of  $\hat{X}_t$  are constructed by  $\hat{\mathbf{x}}_k = \mathbf{x}_k + \delta \mathbf{u}_k$  for  $k = t, \dots, t-m+1$ . Intuitively, adding the random perturbations  $\delta \mathbf{u}_k$  promotes the full row rank property of  $\hat{X}_t$ , thus making  $\hat{X}_{t+1}^\top \hat{X}_{t+1}$  tend to be invertible. This enhances the algorithmic stability of the RESZO method. The magnitude of perturbation is controlled by the value of the smoothing radius parameter  $\delta$ . Since the RESZO method essentially estimates the gradient at the perturbed point, i.e.,  $\nabla f(\hat{\mathbf{x}}) = \nabla f(\mathbf{x} + \delta \mathbf{u}_t)$ , a smaller  $\delta$  generally results in lower gradient estimation bias and promotes convergence precision. Accordingly, rather than selecting a fixed  $\delta$ , we propose an *adaptive  $\delta$  scheme* for the RESZO algorithm in Section 4. The impacts and necessity of incorporating perturbations are further illustrated through numerical experiments in Section 5.2.

### 3.2 Quadratic Regression-Based Single-Point Zeroth-Order Optimization (Q-RESZO)

In addition to fitting a linear model, other more sophisticated surrogate models, such as a *quadratic* function, can be constructed based on available historical function evaluations to further enhance

gradient estimation. At each iteration  $t$ , based on the second-order Taylor expansion at the current perturbed point  $\hat{\mathbf{x}}_t$ , the available function evaluations  $\{f(\hat{\mathbf{x}}_k)\}_{k=0}^t$  can be expressed as:

$$f(\hat{\mathbf{x}}_k) = f(\hat{\mathbf{x}}_t) + \nabla f(\hat{\mathbf{x}}_t)^\top (\hat{\mathbf{x}}_k - \hat{\mathbf{x}}_t) + \frac{1}{2} (\hat{\mathbf{x}}_k - \hat{\mathbf{x}}_t)^\top H_f(\hat{\mathbf{x}}_t) (\hat{\mathbf{x}}_k - \hat{\mathbf{x}}_t) + \epsilon_{t,k}, \quad k=0, 1, \dots, t, \quad (14)$$

where  $H_f(\cdot)$  denotes the Hessian matrix of function  $f$ , and  $\epsilon_{t,k}$  denotes the corresponding higher-order residual term. Accordingly, we can fit a quadratic surrogate function  $f_t^{s2}(\mathbf{x})$  (15) to locally approximate the original function  $f(\mathbf{x})$  in (1):

$$f_t^{s2}(\mathbf{x}) := f(\hat{\mathbf{x}}_t) + \mathbf{g}_t^\top (\mathbf{x} - \hat{\mathbf{x}}_t) + \frac{1}{2} (\mathbf{x} - \hat{\mathbf{x}}_t)^\top \text{diag}(\mathbf{h}_t) (\mathbf{x} - \hat{\mathbf{x}}_t) + c_t. \quad (15)$$

Here, we use the diagonal matrix  $\text{diag}(\mathbf{h}_t)$  with vector  $\mathbf{h}_t \in \mathbb{R}^d$  to approximate the Hessian matrix, which reduces the number of variables for fitting. Similarly, the recursive linear regression in a sliding window is employed, which uses only the latest  $m$  function evaluations  $\{\hat{\mathbf{x}}_{t-i+1}, f(\hat{\mathbf{x}}_{t-i+1})\}_{i=1}^m$  to fit the quadratic surrogate model at each iteration  $t$ .

Then, we solve the following least squares problem (16) to obtain the coefficients  $(\mathbf{g}_t, \mathbf{h}_t, c_t)$ :

$$\min_{\mathbf{g}_t, \mathbf{h}_t, c_t} \sum_{i=1}^m \left[ f_t^{s2}(\hat{\mathbf{x}}_{t-i+1}) - f(\hat{\mathbf{x}}_{t-i+1}) \right]^2 \implies \begin{bmatrix} \mathbf{g}_t \\ \mathbf{h}_t \\ c_t \end{bmatrix} = (\tilde{X}_t^\top \tilde{X}_t)^\dagger \tilde{X}_t^\top \mathbf{y}_t, \quad (16)$$

where  $\odot$  denotes the element-wise multiplication of two column vectors, and

$$\tilde{X}_t := \begin{bmatrix} \Delta_{t,1}^x{}^\top & \frac{1}{2} (\Delta_{t,1}^x \odot \Delta_{t,1}^x)^\top & 1 \\ \Delta_{t,2}^x{}^\top & \frac{1}{2} (\Delta_{t,2}^x \odot \Delta_{t,2}^x)^\top & 1 \\ \vdots & \vdots & \vdots \\ \Delta_{t,m}^x{}^\top & \frac{1}{2} (\Delta_{t,m}^x \odot \Delta_{t,m}^x)^\top & 1 \end{bmatrix} \in \mathbb{R}^{m \times (2d+1)}, \quad \mathbf{y}_t := \begin{bmatrix} \Delta_{t,1}^f \\ \Delta_{t,2}^f \\ \vdots \\ \Delta_{t,m}^f \end{bmatrix} \in \mathbb{R}^m. \quad (17)$$

Accordingly, our proposed **Quadratic Regression-based Single-point Zeroth-order Optimization (Q-RESZO)** method for solving problem (1) follows the same framework as the L-RESZO method (i.e., Algorithm 1), except that it solves for  $(\mathbf{g}_t, \mathbf{h}_t, c_t)$  via (16) in Step 7 and performs the iterative update by (18) with the gradient estimator  $\nabla f_t^{s2}(\mathbf{x})$  in Step 8.

$$\mathbf{x}_{t+1} = \mathbf{x}_t - \eta \nabla f_t^{s2}(\mathbf{x}_t) = \mathbf{x}_t - \eta (\mathbf{g}_t - \delta \mathbf{h}_t \odot \mathbf{u}_t). \quad (18)$$

Additionally, the RESZO algorithms presented above are designed for solving unconstrained optimization problems as formulated in (1); nevertheless, they can be readily extended to constrained optimization problems using projection techniques [22] and primal-dual algorithms [23].

## 4 Theoretical Convergence Analysis

This section provides non-asymptotic convergence analysis, and we focus on the L-RESZO method. Throughout the analysis, we utilize the notation  $[N] := \{1, 2, \dots, N\}$ . We also denote  $\xi_t := \mathbf{g}_t - \nabla f(\mathbf{x}_t)$  to represent the gradient estimation error at an iteration  $t$ .

Throughout our analysis, we use the following standard assumption on the smoothness of the function  $f$ .

**Assumption 1.** The function  $f$  is  $L$ -smooth, i.e.,  $\|\nabla f(\mathbf{x}) - \nabla f(\mathbf{y})\| \leq L\|\mathbf{x} - \mathbf{y}\|$ ,  $\forall \mathbf{x}, \mathbf{y} \in \mathbb{R}^d$ .

For convenience, throughout the analysis, we will study the case where we do not include an intercept  $c_t$ . In this case, the approximate gradient  $\mathbf{g}_t$  is the solution to the equation (19):

$$\mathbf{g}_t = (S_t S_t^\top)^\dagger S_t \Delta_t^f, \quad S_t^\top := \begin{bmatrix} (\hat{\mathbf{x}}_{t-1} - \hat{\mathbf{x}}_t)^\top \\ (\hat{\mathbf{x}}_{t-2} - \hat{\mathbf{x}}_t)^\top \\ \vdots \\ (\hat{\mathbf{x}}_{t-m+1} - \hat{\mathbf{x}}_t)^\top \end{bmatrix}, \quad \Delta_t^f := \begin{bmatrix} f(\hat{\mathbf{x}}_{t-1}) - f(\hat{\mathbf{x}}_t) \\ f(\hat{\mathbf{x}}_{t-2}) - f(\hat{\mathbf{x}}_t) \\ \vdots \\ f(\hat{\mathbf{x}}_{t-m+1}) - f(\hat{\mathbf{x}}_t) \end{bmatrix}, \quad (19)$$

where  $S_t^\top \in \mathbb{R}^{(m-1) \times d}$ ,  $\Delta_t^f \in \mathbb{R}^{m-1}$ .

Inspired by our theoretical analysis, we propose an *adaptive  $\delta$  scheme*, given by (20), to enhance convergence precision:

$$\text{(Adaptive } \delta \text{ Scheme)} : \quad \delta_t = \eta \|\mathbf{g}_{t-1}\|, \quad (20)$$

where the smoothing radius parameter  $\delta_t$  at each iteration  $t$  is adaptively adjusted based on the norm of the last gradient estimate  $\mathbf{g}_{t-1}$ .

In our analysis, we will study the L-RESZO algorithm that employs this adaptive  $\delta$  scheme, and numerical experiments on this scheme are performed in Section 5.2. We also make the following assumption on the regression procedure.

**Assumption 2.** Suppose  $\mathbf{g}_t$  is as defined in (19). We assume that for any  $t \geq m$ ,

$$\|\mathbf{g}_t - \nabla f(\hat{\mathbf{x}}_t)\| \leq C_d \frac{L}{2} \max_{i=1:m-1} \|\hat{\mathbf{x}}_{t-i} - \hat{\mathbf{x}}_t\|, \quad (21)$$

for some constant  $C_d > 0$  depending on the dimension  $d$  and smoothing radius sequence  $\{\delta_t\}_t$ .

Assumption 2 bounds the error of the approximate gradient by the distance between points used in the regression  $\hat{\mathbf{x}}_{t-i}$  and the current point  $\hat{\mathbf{x}}$ ; for clarity, we note that the error  $\mathbf{g}_t - \nabla f(\hat{\mathbf{x}}_t)$  that appears in (21) is distinct from  $\xi_t := \mathbf{g}_t - \nabla f(\mathbf{x}_t)$ , since the former is the bias compared to the gradient at the perturbed point while the latter is the bias compared to the gradient at the actual iterate of the algorithm. While this assumption may appear unmotivated, we show in Appendix A.1 that it holds for  $L$ -smooth functions when  $d = 1$  with  $C_d = 1$ . For general cases of  $d$ , Appendix C presents empirical evidence suggesting that the factor  $C_d$  in Assumption 2 scales in the order of  $\mathcal{O}(\sqrt{d})$  under the adaptive  $\delta_t$  scheme in (20). While establishing a theoretical bound for  $C_d$  is desired, it remains very challenging due to the technical difficulties discussed in Appendix A.1.1.

Before deriving our theoretical convergence results, we first specify the following condition on the initial  $\tilde{\eta}$ , the step-size during the initial update phase (before regression), which states that it should be sufficiently small in a certain sense. Our results later will all require  $\tilde{\eta}$  to satisfy this condition.

**Condition 1.** Recall that  $\tilde{\eta}$  is the step-size of RESZO during the initial update phase (before regression). We pick  $\tilde{\eta}$  such that for any  $t \in \{0, 1, \dots, m-1\}$ , it satisfies<sup>1</sup>

$$\|\mathbf{x}_{t+1} - \mathbf{x}_t\| = \|\tilde{\eta} \mathbf{g}_t\| \leq 2\tilde{\eta} \|\nabla f(\mathbf{x}_t)\|, \quad (22)$$

where  $\mathbf{g}_t$  denotes the estimator of  $\nabla f(\mathbf{x}_t)$  computed using the RSZO method in (3).

<sup>1</sup>We note that this is a relatively mild condition, and that we expect this to hold for any  $\tilde{\eta}$  sufficiently small.

We proceed with introducing our theoretical results. Our analysis is underpinned by the following key technical result, which bounds the gradient approximation error in terms of the norm of the true gradient. To be precise, we show that for any  $0 < c < 1$ , we can inductively guarantee that the gradient estimation bias  $\|\xi_t\|$  always satisfies  $\|\xi_t\| \leq c\|\nabla f(\mathbf{x}_t)\|$  for all  $t \geq m$ .

**Lemma 1.** *Suppose that Assumptions 1 and 2 hold. Suppose  $2 \leq m = \mathcal{O}(d)$ . Suppose we pick  $\tilde{\eta}$  such that it satisfies Condition 1. Then, for any  $0 < c < 1$ , by picking  $\eta = C \frac{1}{dC_d L}$  for some sufficiently small absolute constant  $C > 0$ , we can ensure that*

$$\|\xi_t\| = \|\mathbf{g}_t - \nabla f(\mathbf{x}_t)\| \leq c\|\nabla f(\mathbf{x}_t)\|$$

for any  $t \geq m$ .

We provide a brief proof sketch here, deferring proof details to Appendix A.2. The proof consists of three key steps:

1. First, utilizing Assumption 2 and the adaptive smoothing radius selection, we can bound the gradient estimation error  $\xi_t := \mathbf{g}_t - \nabla f(x_t)$  as

$$\|\xi_t\| \leq \mathcal{O}(C_d L) \sum_{j=1}^m \|\mathbf{x}_{t-j+1} - \mathbf{x}_{t-j}\|, \quad (23)$$

i.e. relate the gradient estimation error to a sum of the increments in the past  $m$  updates.

2. Next, via an inductive argument (utilizing our condition on the initial step-size  $\tilde{\eta}$ ), for any  $t \geq m$  and  $j \in [m]$ , we show that we can always bound the one-step increment  $\|\mathbf{x}_{t-j+1} - \mathbf{x}_{t-j}\|$  as

$$\|\mathbf{x}_{t-j+1} - \mathbf{x}_{t-j}\| \leq 2\eta\|\nabla f(\mathbf{x}_{t-j})\|, \quad (24)$$

i.e. the size of each update can be bounded in terms of the step-size times the norm of the gradient at that step.

3. Utilizing a simple technical result (Lemma 5 in the Appendix A.2), we can show that whenever (24) holds, with an appropriate choice of  $\eta$ , the gradient norm changes only by an  $O(1)$  multiplicative constant across  $m$  iterations. Then, combining this fact with (23) and (24), we have that

$$\begin{aligned} \|\xi_t\| &\leq \mathcal{O}(C_d L) \sum_{j=1}^m \|\mathbf{x}_{t-j+1} - \mathbf{x}_{t-j}\| \\ &\leq \mathcal{O}(C_d L)\eta \sum_{j=1}^m \|\nabla f(\mathbf{x}_{t-j})\| \\ &\leq \mathcal{O}(C_d L)\eta \sum_{j=1}^m \|\nabla f(\mathbf{x}_t)\|. \end{aligned}$$

Using the condition that  $m = \mathcal{O}(d)$ , it follows then that for any  $0 < c < 1$ , by selecting  $\eta = \frac{C}{dC_d L}$  for an appropriately small constant  $C > 0$ , we can ensure that

$$\|\xi_t\| \leq c\|\nabla f(\mathbf{x}_t)\|,$$

as desired.

With Lemma 1 in hand, we can guarantee the following function value improvement per step.

**Lemma 2.** *Suppose that Assumptions 1 and 2 hold. Suppose  $2 \leq m = \mathcal{O}(d)$ . Suppose we pick  $\tilde{\eta}$  such that it satisfies Condition 1. Then, by picking  $\eta = C \frac{1}{dC_d L}$  for some sufficiently small absolute constant  $C > 0$ , we can ensure that*

$$f(\mathbf{x}_{t+1}) - f(\mathbf{x}_t) \leq -\frac{\eta}{8} \|\nabla f(\mathbf{x}_t)\|^2$$

for any  $t \geq m$ .

*Proof.* Consider any positive integer  $t \geq m$ . Fix any  $0 < c < 1$ . By our assumptions, applying Lemma 1, we find that there exists a sufficiently small absolute constant  $C > 0$  such that when  $\eta = \frac{C}{dC_d L}$ , we have

$$\|\xi_t\| \leq c \|\nabla f(\mathbf{x}_t)\|$$

for any  $t \geq m$ .

Next, observe that

$$\begin{aligned} & f(\mathbf{x}_{t+1}) - f(\mathbf{x}_t) \\ & \stackrel{(i)}{\leq} -\eta \langle \nabla f(\mathbf{x}_t), \mathbf{g}_t \rangle + \frac{L}{2} \|\eta \mathbf{g}_t\|^2 \\ & = -\eta \langle \nabla f(\mathbf{x}_t), \nabla f(\mathbf{x}_t) \rangle - \eta \langle \nabla f(\mathbf{x}_t), \mathbf{g}_t - \nabla f(\mathbf{x}_t) \rangle + \frac{L}{2} \|\eta(\mathbf{g}_t - \nabla f(\mathbf{x}_t) + \nabla f(\mathbf{x}_t))\|^2 \\ & \stackrel{(ii)}{\leq} -\eta \|\nabla f(\mathbf{x}_t)\|^2 + \frac{\eta}{2} (\|\nabla f(\mathbf{x}_t)\|^2 + \|\xi_t\|^2) + \eta^2 L (\|\nabla f(\mathbf{x}_t)\|^2 + \|\xi_t\|^2) \\ & \leq -\frac{\eta}{4} \|\nabla f(\mathbf{x}_t)\|^2 + \eta \|\xi_t\|^2, \end{aligned} \tag{25}$$

where (i) follows by  $L$ -smoothness of  $f$ , (ii) follows by application of Young's equality as well as the notation  $\xi_t := \mathbf{g}_t - \nabla f(\mathbf{x}_t)$ , and the final inequality follows by choosing  $\eta \leq \frac{1}{4L}$ .

Thus, continuing from (25), by picking  $c$  to be smaller than  $\frac{1}{\sqrt{8}}$ , such that

$$\|\xi_t\| \leq \frac{1}{\sqrt{8}} \|\nabla f(\mathbf{x}_t)\|,$$

we find that

$$\begin{aligned} f(\mathbf{x}_{t+1}) - f(\mathbf{x}_t) & \leq -\frac{\eta}{4} \|\nabla f(\mathbf{x}_t)\|^2 + \eta \|\xi_t\|^2 \\ & \leq -\frac{\eta}{4} \|\nabla f(\mathbf{x}_t)\|^2 + \frac{\eta}{8} \|\nabla f(\mathbf{x}_t)\|^2 \\ & \leq -\frac{\eta}{8} \|\nabla f(\mathbf{x}_t)\|^2, \end{aligned}$$

as desired. □

Equipped with Lemma 2, we can easily show by standard arguments that the algorithm converges at a sublinear rate for smooth nonconvex functions, and at a linear rate for smooth strongly convex functions. We defer proof details to Appendix A.2.

**Theorem 1.** *Suppose Assumptions 1 and 2 hold. Suppose  $2 \leq m = \mathcal{O}(d)$ . Suppose we pick  $\tilde{\eta}$  such that it satisfies Condition 1. Then, by picking  $\eta = C \frac{1}{dC_d L}$  for some sufficiently small absolute constant  $C > 0$ , for any  $T > m$ , the L-RESZO algorithm achieves*

$$\frac{1}{T} \sum_{t=m}^{T-1} \|\nabla f(\mathbf{x}_t)\|^2 \leq \mathcal{O} \left( \frac{dC_d L(f(\mathbf{x}_m) - f^*)}{T} \right).$$

This convergence rate scales as  $\mathcal{O}(\frac{dC_d L}{T})$ , decaying at the rate  $1/T$ . When the term  $C_d$  is on the order of  $\sqrt{d}$  (as observed empirically under the adaptive choice of  $\delta_t = \eta \|\mathbf{g}_{t-1}\|$  (20); see Appendix C for more details), this matches the standard convergence rate for two-point ZO of smooth nonconvex functions, up to a factor of  $\sqrt{d}$ .

Next, we present a linear convergence rate for strongly convex functions.

**Theorem 2.** *Suppose Assumptions 1 and 2 hold. Suppose  $2 \leq m = \mathcal{O}(d)$ . Suppose we pick  $\tilde{\eta}$  such that it satisfies Condition 1. Then, by picking  $\eta = C \frac{1}{dC_d L}$  for some sufficiently small absolute constant  $C > 0$ , for any  $T > m$ , the L-RESZO algorithm achieves*

$$f(\mathbf{x}_T) - f^* \leq \left( 1 - \mathcal{O} \left( \frac{\mu}{C_d L d} \right) \right)^{T-m} (f(\mathbf{x}_m) - f^*).$$

Theorem 2 shows that with the adaptive  $\delta_t$  sequence, the L-RESZO achieves a linear convergence rate that is worse than that of two-point ZO methods for strongly convex functions only by a factor of  $C_d$ . We provide strong empirical evidence in Appendix C that  $C_d$  scales as  $\mathcal{O}(\sqrt{d})$  for both ridge and logistic regression problems. This implies that, for these problems, the theoretical linear convergence rate of L-RESZO is worse than that of two-point ZO only by a factor of  $\sqrt{d}$ .

## 5 Numerical Experiments

This section demonstrates the performance of the proposed RESZO methods in comparison with classic ZO methods through numerical experiments<sup>2</sup>, and studies the impact of adding perturbations.

### 5.1 Comparison with Classic ZO Methods

We compare the performance of the proposed L-RESZO (i.e., Algorithm 1), Q-RESZO (18) methods with the RSZO (3) and TZO (4) methods across four optimization tasks, including ridge regression, logistic regression, Rosenbrock function minimization, and neural networks training.

**Case (a) Ridge Regression.** Consider solving the ridge regression problem (26) [24]:

$$\min_{\mathbf{x} \in \mathbb{R}^d} f(\mathbf{x}) = \frac{1}{2} \|\mathbf{y} - H\mathbf{x}\|_2^2 + \frac{\lambda}{2} \|\mathbf{x}\|_2^2. \quad (26)$$

In our experiments, each entry of the matrix  $H \in \mathbb{R}^{N \times d}$  is independently drawn from the standard Gaussian distribution  $\mathcal{N}(0, 1)$ . The column vector  $\mathbf{y} \in \mathbb{R}^N$  is constructed by letting  $\mathbf{y} = \frac{1}{2} H \mathbf{1}_d + \boldsymbol{\epsilon}$ , where  $\mathbf{1}_d$  denotes the  $d$ -dimensional all-ones vector and  $\boldsymbol{\epsilon} \sim \mathcal{N}(\mathbf{0}, 0.1\mathbf{I})$  represents the additive Gaussian noise. The regularization parameter is fixed as  $\lambda = 0.1$ , and the initial point is set to  $\mathbf{x}_0 = \mathbf{0}_d$ . We set  $N = 1000$  and the problem dimension  $d = 100$ .

<sup>2</sup>All numerical experiments are coded in Matlab and implemented in a computing environment with Intel(R) Core(TM) i7-1185G7 CPUs running at 3.00 GHz and with 16 GB RAM.

**Case (b) Logistic Regression.** Consider solving the logistic regression problem (27) [24]:

$$\min_{\mathbf{x} \in \mathbb{R}^d} f(\mathbf{x}) = \frac{1}{2} \sum_{i=1}^N \log(1 + \exp(-y_i \cdot \mathbf{s}_i^\top \mathbf{x})) + \frac{\lambda}{2} \|\mathbf{x}\|_2^2, \quad (27)$$

where  $\mathbf{s}_i \in \mathbb{R}^d$  is one of the data samples,  $y_i \in \{-1, 1\}$  is the corresponding class label, and  $N = 1000$  is the sample size. In our experiments, each element of a data sample  $\mathbf{s}_i$  is independently drawn from the uniform distribution  $\text{Unif}([-1, 1])$ , and the corresponding label is computed as  $y_i = \text{sign}(\frac{1}{2} \mathbf{s}_i^\top \mathbf{1}_d)$ . The regularization parameter is fixed as  $\lambda = 0.1$ , and we set  $d = 100$ .

**Case (c) Rosenbrock Function.** Consider minimizing the nonconvex Rosenbrock function (28):

$$\min_{\mathbf{x} \in \mathbb{R}^d} f(\mathbf{x}) = \sum_{i=1}^d \left[ 100((x_i + 1)^2 - x_{i+1} - 1)^2 + x_i^2 \right], \quad (28)$$

which is a well-known benchmark problem for numerical optimization [25]. The global optimal solution and objective value are  $\mathbf{x}^* = \mathbf{0}$  and  $f^* = 0$ . We set  $d = 200$  and the initial point  $\mathbf{x}_0 = 0.5 \mathbf{1}_d$ .

**Case (d) Neural Network Training.** Consider training a three-layer fully connected neural network by minimizing the loss function (29):

$$\min_{\mathbf{x} \in \mathbb{R}^d} f(\mathbf{x}) = \sum_{i=1}^N \left[ \mathbf{w}_o^\top \sigma(W_3 \sigma(W_2 \sigma(W_1 \mathbf{s}_i + \mathbf{b}_1) + \mathbf{b}_2) + \mathbf{b}_3) - y_i \right]^2, \quad (29)$$

where the decision variable is  $\mathbf{x} := (W_1, W_2, W_3, \mathbf{b}_1, \mathbf{b}_2, \mathbf{b}_3, \mathbf{w}_o)$ , and  $\sigma(\cdot)$  denotes the Sigmoid activation function. Let  $\mathbf{s}_i \in \mathbb{R}^n$  and  $y_i \in \mathbb{R}$  be the input and output of each sample  $i$  with  $n = 6$ . Thus, the problem dimension is  $d = 3n^2 + 4n = 132$ . We set the sample size to  $N = 500$ . Each sample input  $\mathbf{s}_i$  is randomly drawn from the standard Gaussian distribution  $\mathcal{N}(0, 1)$ , and the corresponding output is computed by the neural network with ground truth  $\mathbf{x}^*$ , where each entry of  $\mathbf{x}^*$  is randomly generated from  $\mathcal{N}(0, 1)$ . Let the initial point be  $\mathbf{x}_0 = \mathbf{x}^* + \boldsymbol{\varepsilon}$ , and each entry of  $\boldsymbol{\varepsilon}$  is randomly drawn from the uniform distribution  $\text{Unif}([-1, 1])$ .

For each ZO method, we optimize the stepsize  $\eta$  and the smoothing radius  $\delta$  via grid search to achieve the fastest convergence, and the selected parameters are summarized in Table 2. The same sample size  $m$  is used for L-RESZO and Q-RESZO, which is set to 110, 110, 210, and 6 in Cases (a)-(d)<sup>3</sup>, respectively. For each of the four optimization tasks described above, we run each ZO method 100 times and calculate the mean and 80%-confidence interval (CI) of the optimality gap  $f(\mathbf{x}) - f^*$ . Figure 1 illustrates the convergence results using the TZO, RSZO, L-RESZO, and Q-RESZO methods, evaluated based on the number of function queries.

As shown in Figure 1, the proposed L-RESZO and Q-RESZO methods outperform the TZO method in terms of function query complexity across all test cases and converge significantly faster than the RSZO method. Regarding iteration complexity, L-RESZO and Q-RESZO achieve a convergence rate comparable to that of TZO, which is consistent with our theoretical analysis. However, since L-RESZO and Q-RESZO require only one function query per iteration, they are approximately twice as fast as TZO with respect to function query complexity. Q-RESZO exhibits slightly faster convergence than L-RESZO, attributable to more accurate gradient estimation enabled by quadratic surrogate functions. Nevertheless, TZO ultimately attains higher convergence precision

<sup>3</sup>In Cases (a)-(c), the sample size is chosen as  $m = d + 10$  to be slightly larger than the problem dimension  $d$ . However, in Case (d), a smaller sample size  $m$  yields better convergence, and thus a very small sample size  $m = 6$  is used. It implies that, for certain problems, a small sample size might be preferable and only few recent function evaluations are needed to construct an effective gradient estimate with the proposed RESZO method.

Table 2: Selected parameters of smoothing radius  $\delta$  and stepsize  $\eta$  for the ZO methods.

Methods	Ridge Reg.		Logistic Reg.		Rosenbrock Func.		Neural Network	
	$\delta$	$\eta$	$\delta$	$\eta$	$\delta$	$\eta$	$\delta$	$\eta$
TZO	0.002	$1.1 \times 10^{-5}$	0.01	$1.6 \times 10^{-3}$	0.01	$4.5 \times 10^{-6}$	0.01	$3.8 \times 10^{-4}$
RSZO	0.2	$2.5 \times 10^{-6}$	2	$5 \times 10^{-4}$	0.5	$2 \times 10^{-6}$	0.05	$1.1 \times 10^{-4}$
L-RESZO	0.002	$8 \times 10^{-6}$	0.1	$2 \times 10^{-3}$	0.02	$4.2 \times 10^{-6}$	0.001	$1.7 \times 10^{-3}$
Q-RESZO	0.002	$1.6 \times 10^{-5}$	0.01	$5 \times 10^{-3}$	0.02	$1 \times 10^{-5}$	0.001	$1.7 \times 10^{-3}$

than L-RESZO and Q-RESZO. As illustrated in the next subsection, the convergence precision of L-RESZO and Q-RESZO is controlled by the smoothing radius  $\delta$ .

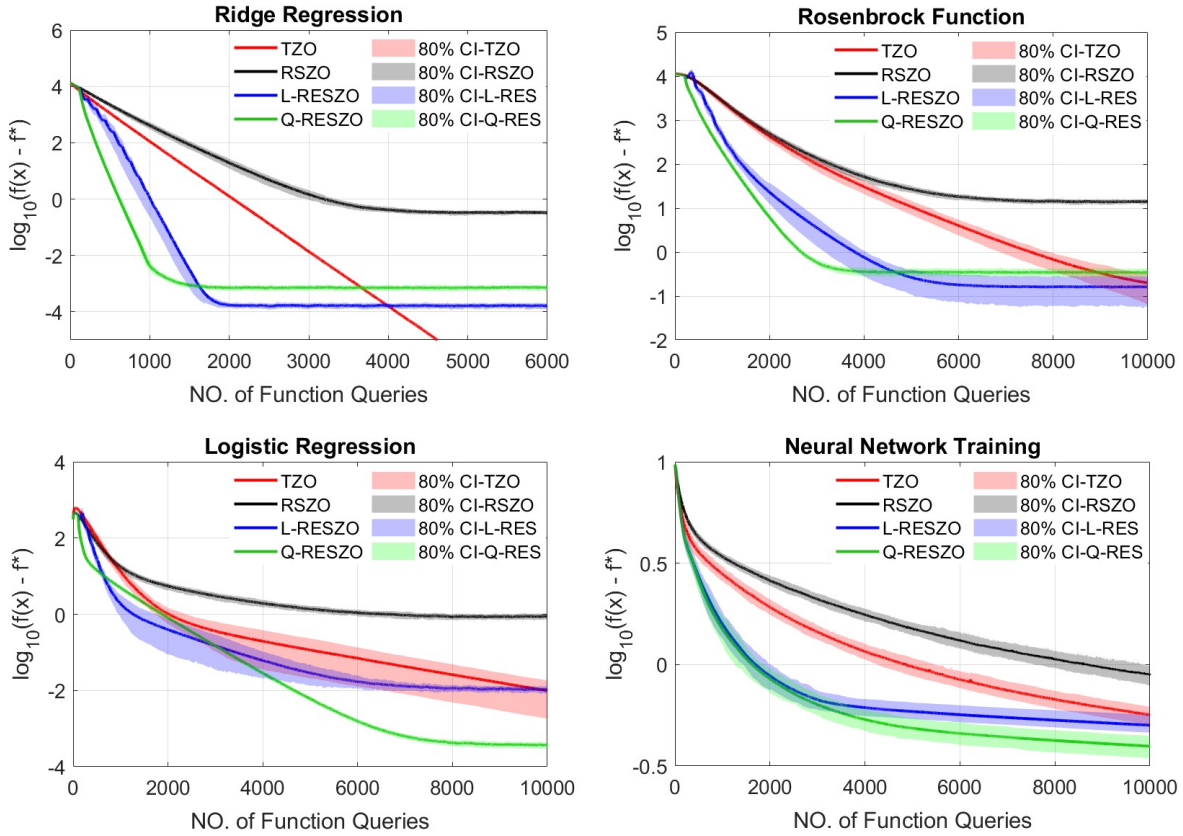


Figure 1: The convergence results of applying the TZO (4), RSZO (3), L-RESZO (Algorithm 1) and Q-RESZO (18) methods to solve ridge regression (26), logistic regression (27), Rosenbrock function minimization (28), and neural network training (29).

## 5.2 Impact of Random Perturbations on RESZO

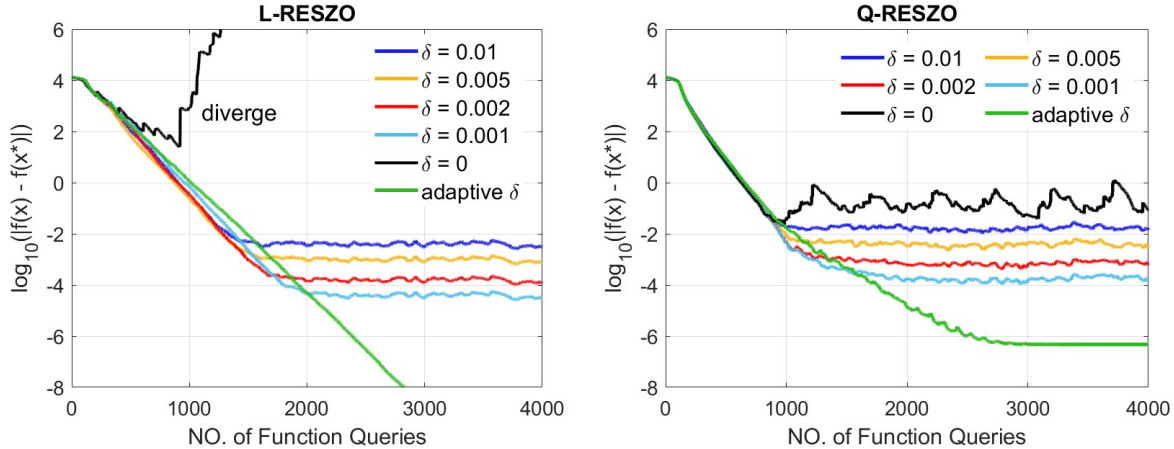


Figure 2: Convergence of L-RESZO and Q-RESZO for solving the ridge regression problem (26) under different levels of perturbations and using the adaptive  $\delta$  scheme (20).

To analyze the impact of perturbations added for function evaluations, we test the proposed L-RESZO and Q-RESZO methods under varying levels of the smoothing radius  $\delta$  when solving the ridge regression problem (26). The experimental settings remain the same as those described in the previous subsection. Specifically, the smoothing radius  $\delta$  is progressively reduced from 0.01, 0.005, 0.002, 0.001, to zero (no perturbation), and we also perform the adaptive smoothing radius scheme given by (20). The test results are illustrated in Figure 2. It is observed that a smaller smoothing radius  $\delta$  leads to improved convergence precision. That is because the RESZO method essentially estimates the gradient at the perturbed point, i.e.,  $\nabla f(\hat{x}) = \nabla f(x + \delta u_t)$ , and thus a smaller  $\delta$  results in lower estimation errors. However, the introduction of random perturbations is necessary for the stability of RESZO. Figure 2 shows that, when no perturbation is added ( $\delta = 0$ ), the Q-RESZO method exhibits large oscillations and poor convergence precision, while the L-RESZO method even diverges. Moreover, corroborating our theoretical results, our adaptive  $\delta$  scheme given by (20) can effectively enhance convergence precision by adjusting  $\delta$  based on the updated gradient estimate.

## 6 Conclusion

In this paper, we propose a novel yet simple Single-point Zeroth-order Optimization (SZO) framework, termed Regression-Based SZO (RESZO), which significantly improves gradient estimation by leveraging historical function evaluations from previous iterations. We theoretically establish that the RESZO method achieves convergence rates comparable to those of the two-point ZO method for both smooth nonconvex and strongly convex functions. Moreover, extensive numerical experiments demonstrate that RESZO not only matches but achieves approximately twice as fast convergence as the two-point ZO method in terms of function query complexity in all test cases. To the best of our knowledge, this is the first work to present single-point ZO that achieves a comparable convergence rate to two-point ZO and empirically outperforms it.

**Limitations.** Despite showing comparable convergence rates to two-point ZO, the theoretical analysis in this paper can be further enhanced by (i) rigorously bounding the term  $C_d$  in Assumption 2 and (ii) improving the convergence rate bounds to exactly match those of two-point ZO, as observed in practice. Additionally, this work focuses exclusively on the noiseless setting; extending the analysis

and algorithms to handle noisy function evaluations would better reflect practical scenarios. Future studies can be conducted to explore various strategies to further improve the RESZO framework, such as fitting more advanced surrogate functions, incorporating weighting schemes for historical function evaluations, adopting adaptive stepsize rules, and integrating trust region methods, etc.

## References

- [1] Xin Chen, Jorge I Poveda, and Na Li. Safe model-free optimal voltage control via continuous-time zeroth-order methods. In *2021 60th IEEE Conference on Decision and Control (CDC)*, pages 4064–4070. IEEE, 2021.
- [2] Yue Chen, Andrey Bernstein, Adithya Devraj, and Sean Meyn. Model-free primal-dual methods for network optimization with application to real-time optimal power flow. In *2020 American Control Conference (ACC)*, pages 3140–3147. IEEE, 2020.
- [3] Dhruv Malik, Ashwin Pananjady, Kush Bhatia, Koulik Khamaru, Peter Bartlett, and Martin Wainwright. Derivative-free methods for policy optimization: Guarantees for linear quadratic systems. In *The 22nd International Conference on Artificial Intelligence and Statistics*, pages 2916–2925. PMLR, 2019.
- [4] Yingying Li, Yujie Tang, Runyu Zhang, and Na Li. Distributed reinforcement learning for decentralized linear quadratic control: A derivative-free policy optimization approach. *arXiv preprint arXiv:1912.09135*, 2019.
- [5] Aochuan Chen, Yimeng Zhang, Jinghan Jia, James Diffenderfer, Jiancheng Liu, Konstantinos Parasyris, Yihua Zhang, Zheng Zhang, Bhavya Kailkhura, and Sijia Liu. Deepzero: Scaling up zeroth-order optimization for deep model training. *arXiv preprint arXiv:2310.02025*, 2023.
- [6] Pin-Yu Chen, Huan Zhang, Yash Sharma, Jinfeng Yi, and Cho-Jui Hsieh. Zoo: Zeroth order optimization based black-box attacks to deep neural networks without training substitute models. In *Proceedings of the 10th ACM workshop on artificial intelligence and security*, pages 15–26, 2017.
- [7] Sijia Liu, Pin-Yu Chen, Bhavya Kailkhura, Gaoyuan Zhang, Alfred O Hero III, and Pramod K Varshney. A primer on zeroth-order optimization in signal processing and machine learning: Principals, recent advances, and applications. *IEEE Signal Processing Magazine*, 37(5):43–54, 2020.
- [8] Yurii Nesterov and Vladimir Spokoiny. Random gradient-free minimization of convex functions. *Foundations of Computational Mathematics*, 17(2):527–566, 2017.
- [9] Abraham D. Flaxman, Adam Tauman Kalai, and H. Brendan McMahan. Online convex optimization in the bandit setting: Gradient descent without a gradient. In *Proceedings of the Sixteenth Annual ACM-SIAM Symposium on Discrete Algorithms*, page 385–394, 2005.
- [10] Yan Zhang, Yi Zhou, Kaiyi Ji, and Michael M Zavlanos. A new one-point residual-feedback oracle for black-box learning and control. *Automatica*, page 110006, 2021.
- [11] Xin Chen, Yujie Tang, and Na Li. Improve single-point zeroth-order optimization using high-pass and low-pass filters. In *International Conference on Machine Learning*, pages 3603–3620. PMLR, 2022.

- [12] Ankan Saha and Ambuj Tewari. Improved regret guarantees for online smooth convex optimization with bandit feedback. In *Proceedings of the Fourteenth International Conference on Artificial Intelligence and Statistics*, pages 636–642. JMLR Workshop and Conference Proceedings, 2011.
- [13] Ofer Dekel, Ronen Eldan, and Tomer Koren. Bandit smooth convex optimization: Improving the bias-variance tradeoff. In *NIPS*, pages 2926–2934, 2015.
- [14] Alexander V Gasnikov, Ekaterina A Krymova, Anastasia A Lagunovskaya, Ilnura N Usmanova, and Fedor A Fedorenko. Stochastic online optimization. single-point and multi-point non-linear multi-armed bandits. convex and strongly-convex case. *Automation and Remote Control*, 78(2):224–234, 2017.
- [15] Yan Zhang, Yi Zhou, Kaiyi Ji, and Michael M Zavlanos. A new one-point residual-feedback oracle for black-box learning and control. *Automatica*, 136:110006, 2022.
- [16] Vasili Novitskii and Alexander Gasnikov. Improved exploiting higher order smoothness in derivative-free optimization and continuous bandit. *arXiv preprint arXiv:2101.03821*, 2021.
- [17] Andrew R Conn, Katya Scheinberg, and Luis N Vicente. *Introduction to derivative-free optimization*. SIAM, 2009.
- [18] Albert S Berahas, Liyuan Cao, Krzysztof Choromanski, and Katya Scheinberg. A theoretical and empirical comparison of gradient approximations in derivative-free optimization. *Foundations of Computational Mathematics*, 22(2):507–560, 2022.
- [19] Xiaoxing Wang, Xiaohan Qin, Xiaokang Yang, and Junchi Yan. Relizo: Sample reusable linear interpolation-based zeroth-order optimization. *Advances in Neural Information Processing Systems*, 37:15070–15096, 2024.
- [20] Jeffrey Larson, Matt Menickelly, and Stefan M Wild. Derivative-free optimization methods. *Acta Numerica*, 28:287–404, 2019.
- [21] Chun Yuan Deng. A generalization of the sherman–morrison–woodbury formula. *Applied Mathematics Letters*, 24(9):1561–1564, 2011.
- [22] Xin Chen, Jorge I Poveda, and Na Li. Continuous-time zeroth-order dynamics with projection maps: Model-free feedback optimization with safety guarantees. *IEEE Transactions on Automatic Control*, 2025.
- [23] Xin Chen, Jorge I Poveda, and Na Li. Model-free feedback constrained optimization via projected primal-dual zeroth-order dynamics. *arXiv preprint arXiv:2206.11123*, 2022.
- [24] César A Uribe, Soomin Lee, Alexander Gasnikov, and Angelia Nedić. A dual approach for optimal algorithms in distributed optimization over networks. In *2020 Information Theory and Applications Workshop (ITA)*, pages 1–37. IEEE, 2020.
- [25] Yun-Wei Shang and Yu-Huang Qiu. A note on the extended rosenbrock function. *Evolutionary Computation*, 14(1):119–126, 2006.

# A Proofs for Theoretical Convergence Analysis

## A.1 More on Assumption 2

To facilitate our analysis, we first show the following result which provides an alternative characterization of the approximation error term  $\|\mathbf{g}_t - \nabla f(\hat{\mathbf{x}}_t)\|$  that appears in Assumption 2.

**Lemma 3.** *Suppose  $\mathbf{g}_t$  is defined as in (19), i.e.*

$$\mathbf{g}_t = (S_t S_t^\top)^\dagger S_t \Delta_t^f, \quad S_t^\top := \begin{bmatrix} (\hat{\mathbf{x}}_{t-1} - \hat{\mathbf{x}}_t)^\top \\ (\hat{\mathbf{x}}_{t-2} - \hat{\mathbf{x}}_t)^\top \\ \vdots \\ (\hat{\mathbf{x}}_{t-m+1} - \hat{\mathbf{x}}_t)^\top \end{bmatrix}, \quad \Delta_t^f := \begin{bmatrix} f(\hat{\mathbf{x}}_{t-1}) - f(\hat{\mathbf{x}}_t) \\ f(\hat{\mathbf{x}}_{t-2}) - f(\hat{\mathbf{x}}_t) \\ \vdots \\ f(\hat{\mathbf{x}}_{t-m+1}) - f(\hat{\mathbf{x}}_t) \end{bmatrix}.$$

Define the errors of the first-order Taylor expansion as:

$$\boldsymbol{\epsilon}_t := \begin{bmatrix} f(\hat{\mathbf{x}}_{t-1}) - (f(\hat{\mathbf{x}}_t) + \langle \nabla f(\hat{\mathbf{x}}_t), \hat{\mathbf{x}}_{t-1} - \hat{\mathbf{x}}_t \rangle) \\ \vdots \\ f(\hat{\mathbf{x}}_{t-m+1}) - (f(\hat{\mathbf{x}}_t) + \langle \nabla f(\hat{\mathbf{x}}_t), \hat{\mathbf{x}}_{t-m+1} - \hat{\mathbf{x}}_t \rangle) \end{bmatrix}. \quad (30)$$

Suppose  $S_t S_t^\top \in \mathbb{R}^{d \times d}$  is invertible. Then,

$$\mathbf{g}_t - \nabla f(\hat{\mathbf{x}}_t) = (S_t S_t^\top)^{-1} S_t \boldsymbol{\epsilon}_t.$$

*Proof.* Using the assumption that  $S_t S_t^\top \in \mathbb{R}^{d \times d}$  is invertible, we have

$$\begin{aligned} \mathbf{g}_t &= (S_t S_t^\top)^{-1} S_t \Delta_t^f = (S_t S_t^\top)^{-1} S_t \left( S_t^\top \nabla f(\hat{\mathbf{x}}_t) + \boldsymbol{\epsilon}_t \right) \\ &= \nabla f(\hat{\mathbf{x}}_t) + (S_t S_t^\top)^{-1} S_t \boldsymbol{\epsilon}_t, \end{aligned}$$

as desired.  $\square$

We first prove the following result (under a very mild condition stated in (31)) showing that Assumption 2 holds with  $C_d = 1$  in the case  $d = 1$ . Define  $[N] := \{1, 2, \dots, N\}$ .

**Lemma 4.** *Suppose Assumption 1 holds. Suppose  $d = 1$ . Suppose also that there exists some  $i \in [m-1]$  such that*

$$|\hat{\mathbf{x}}_{t,i} - \hat{\mathbf{x}}| > 0. \quad (31)$$

Then, with  $\mathbf{g}_t$  being defined as in (19), for any  $t \geq m$ , Assumption 2 holds with  $C_d = 1$ , i.e.

$$\|\mathbf{g}_t - \nabla f(\hat{\mathbf{x}}_t)\| \leq \frac{L}{2} \max_{i=1:m-1} |\hat{\mathbf{x}}_{t-i} - \hat{\mathbf{x}}|.$$

*Proof.* Note that  $d = 1$ . Since we assume there exists some  $i \in [m-1]$  such that  $|\hat{\mathbf{x}}_{t,i} - \hat{\mathbf{x}}| > 0$ , we know that  $S_t S_t^\top \in \mathbb{R}$  is invertible, satisfying the condition in Lemma 3. Thus, using Lemma 3, we note that the result is equivalent to showing that

$$|(S_t S_t^\top)^{-1} S_t \boldsymbol{\epsilon}_t| \leq \frac{L}{2} \max_{i=1:m-1} |\hat{\mathbf{x}}_{t-i} - \hat{\mathbf{x}}|.$$

Let  $\epsilon_{t,i}$  denote the  $i$ -th entry of  $\boldsymbol{\epsilon}_t \in \mathbb{R}^{m-1}$ . By  $L$ -smoothness of  $f$ , we observe that for any  $i \in [m-1]$ , we have

$$|\epsilon_{t,i}| = |f(\hat{\mathbf{x}}_{t-i}) - (f(\hat{\mathbf{x}}_t) + \langle \nabla f(\hat{\mathbf{x}}_t), \hat{\mathbf{x}}_{t-i} - \hat{\mathbf{x}}_t \rangle)| \leq \frac{L}{2} \|\hat{\mathbf{x}}_{t-i} - \hat{\mathbf{x}}_t\|^2.$$

Using the above result, in the case  $d = 1$ , we observe that

$$\begin{aligned}
|(S_t S_t^\top)^{-1} S_t \epsilon_t| &= \left| \frac{1}{\sum_{i=1}^{m-1} |\hat{\mathbf{x}}_{t-i} - \hat{\mathbf{x}}_t|^2} \sum_{i=1}^{m-1} (\hat{\mathbf{x}}_{t-i} - \hat{\mathbf{x}}_t) \epsilon_{t,i} \right| \\
&\leq \frac{1}{\sum_{i=1}^{m-1} |\hat{\mathbf{x}}_{t-i} - \hat{\mathbf{x}}_t|^2} \max_{i=1:m-1} |\hat{\mathbf{x}}_{t-i} - \hat{\mathbf{x}}_t| \sum_{i=1}^{m-1} |\epsilon_{t,i}| \\
&\leq \frac{1}{\sum_{i=1}^{m-1} |\hat{\mathbf{x}}_{t-i} - \hat{\mathbf{x}}_t|^2} \max_{i=1:m-1} |\hat{\mathbf{x}}_{t-i} - \hat{\mathbf{x}}_t| \sum_{i=1}^{m-1} \frac{L}{2} |\hat{\mathbf{x}}_{t-i} - \hat{\mathbf{x}}_t|^2 \\
&\leq \frac{L}{2} \max_{i=1:m-1} |\hat{\mathbf{x}}_{t-i} - \hat{\mathbf{x}}_t|,
\end{aligned}$$

as desired.  $\square$

### A.1.1 Technical Challenges of Proving Assumption 2 for General Cases with $d > 1$

From Lemma 3, suppose that  $S_t S_t^\top$  is invertible, proving Assumption 2 is equivalent to showing that

$$\|(S_t S_t^\top)^{-1} S_t \epsilon_t\| \leq \frac{C_d L}{2} \max_{i=1:m-1} \|\hat{\mathbf{x}}_{t-i} - \hat{\mathbf{x}}_t\|,$$

for some  $C_d > 0$ . A natural approach to proving the above inequality is to use the standard bound

$$\|(S_t S_t^\top)^{-1} S_t \epsilon_t\| \leq \|(S_t S_t^\top)^{-1}\|_2 \|S_t \epsilon_t\|.$$

However, it is (i) unclear how we might theoretically bound  $\|(S_t S_t^\top)^{-1}\|_2$ , and (ii), empirically, when  $d < m = \mathcal{O}(d)$  regression samples are used, on the ridge regression, we observe that  $\|(S_t S_t^\top)^{-1}\|_2$  scales as<sup>4</sup>

$$\|(S_t S_t^\top)^{-1}\|_2 = \Omega \left( \frac{d^3}{\sum_{i=1}^{m-1} \|\hat{\mathbf{x}}_{t-i} - \hat{\mathbf{x}}_t\|^2} \right).$$

Combining this with the argument in Lemma 4 bounding  $\|\epsilon_{t,i}\|$  as

$$|\epsilon_{t,i}| = |f(\hat{\mathbf{x}}_{t-i}) - (f(\hat{\mathbf{x}}_t) + \langle \nabla f(\hat{\mathbf{x}}_t), \hat{\mathbf{x}}_{t-i} - \hat{\mathbf{x}}_t \rangle)| \leq \frac{L}{2} \|\hat{\mathbf{x}}_{t-i} - \hat{\mathbf{x}}_t\|,$$

it yields

$$\begin{aligned}
\|(S_t S_t^\top)^{-1} S_t \epsilon_t\| &\leq \|(S_t S_t^\top)^{-1}\|_2 \|S_t \epsilon_t\| \\
&\leq \Omega \left( \frac{d^3}{\sum_{i=1}^{m-1} \|\hat{\mathbf{x}}_{t-i} - \hat{\mathbf{x}}_t\|^2} \right) \left\| \sum_{i=1}^{m-1} (\hat{\mathbf{x}}_{t-i} - \hat{\mathbf{x}}_t) \epsilon_{t,i} \right\| \\
&\leq \Omega \left( \frac{d^3}{\sum_{i=1}^{m-1} \|\hat{\mathbf{x}}_{t-i} - \hat{\mathbf{x}}_t\|^2} \right) \max_{i=1:m-1} \|\hat{\mathbf{x}}_{t-i} - \hat{\mathbf{x}}_t\| \sum_{i=1}^{m-1} \frac{L}{2} \|\hat{\mathbf{x}}_{t-i} - \hat{\mathbf{x}}_t\|^2 \\
&\leq \Omega(d^3) \frac{L}{2} \max_{i=1:m-1} \|\hat{\mathbf{x}}_{t-i} - \hat{\mathbf{x}}_t\|,
\end{aligned}$$

<sup>4</sup>We recall that the notation  $\Omega(\cdot)$  is defined as follows: for any non-negative variable  $n$ , saying that a positive function  $f(n)$  is  $\Omega(g(n))$ , where  $g(n)$  is some positive function of  $n$ , means that there exists some absolute constant  $C_1 > 0$  and a number  $n_0$  such that for all  $n \geq n_0$ , we have  $f(n) \geq C_1 g(n) > 0$ .

yielding  $C_d = \Omega(d^3)$ , which as we later demonstrate empirically in Appendix C, vastly overestimates the true size of  $C_d$  that tends to scale as  $\mathcal{O}(\sqrt{d})$ . This suggests that the natural approach of estimating  $C_d$  by first bounding  $\|(S_t S_t^\top)^{-1}\|_2$  does not yield tight bounds; additionally, it is in the first place also non-trivial to theoretically prove an upper bound for  $\|(S_t S_t^\top)^{-1}\|_2$ .

Thus, we regard the task of accurately bounding  $\|(S_t S_t^\top)^{-1} S_t \epsilon_t\|$  as a very challenging theoretical problem which we leave to future work.

## A.2 Proofs for Lemma 1, Theorem 1, and Theorem 2

Throughout the analysis, without loss of generality, we assume that  $C_d \geq 1$ . We also recall what we stated earlier, which is that we will study a variant of the L-RESZO algorithm with an adaptive choice of smoothing radius  $\delta_t$  as (20),

$$\delta_t := \eta \|\mathbf{g}_{t-1}\|.$$

We first prove the following useful helper result, which bounds the change in gradient norm across  $m$  iterations whenever the gradient estimation bias can be bounded in terms of the true gradient norm.

**Lemma 5.** *Suppose Assumption 1 holds. Suppose  $2 \leq m = \mathcal{O}(d)$ . Consider any  $t \geq m$ . Suppose that*

$$\|\mathbf{x}_{j+1} - \mathbf{x}_j\| \leq 2\eta \|\nabla f(\mathbf{x}_j)\| \tag{32}$$

for all  $j < t$ .

Then, by picking  $\eta = \mathcal{O}(\frac{1}{dL})$ , we can ensure that

$$\|\nabla f(\mathbf{x}_{t-j})\| \leq 4\|\nabla f(\mathbf{x}_t)\|$$

for any  $j \in [m]$ .

*Proof.* Consider any  $t \geq m$ , and consider any  $0 \leq j < t$ . Since by assumption

$$\|\mathbf{x}_{j+1} - \mathbf{x}_j\| \leq 2\eta \|\nabla f(\mathbf{x}_j)\|,$$

we have that

$$\|\nabla f(\mathbf{x}_{j+1}) - \nabla f(\mathbf{x}_j)\| \leq L\|\mathbf{x}_{j+1} - \mathbf{x}_j\| \leq 2\eta L\|\nabla f(\mathbf{x}_j)\|, \tag{33}$$

where the first line utilizes  $L$ -smoothness and the second line utilizes our assumption in (32). Continuing, we observe that

$$\begin{aligned} \|\nabla f(\mathbf{x}_j)\| &\leq \|\nabla f(\mathbf{x}_{j+1})\| + \|\nabla f(\mathbf{x}_j) - \nabla f(\mathbf{x}_{j+1})\| \\ &\leq \|\nabla f(\mathbf{x}_{j+1})\| + 2\eta L\|\nabla f(\mathbf{x}_j)\|, \end{aligned}$$

where the first inequality uses triangle inequality and the second inequality follows from (33). Rearranging, we find that

$$\begin{aligned} (1 - 2\eta L)\|\nabla f(\mathbf{x}_j)\| &\leq \|\nabla f(\mathbf{x}_{j+1})\| \\ \implies \|\nabla f(\mathbf{x}_j)\| &\leq \frac{1}{1 - 2\eta L}\|\nabla f(\mathbf{x}_{j+1})\|. \end{aligned}$$

Suppose we pick  $\eta = \frac{1}{2mL}$ . Then, continuing, we find that

$$\begin{aligned}\|\nabla f(\mathbf{x}_j)\| &\leq \frac{1}{1-2\eta L}\|\nabla f(\mathbf{x}_{j+1})\| \\ &\leq \frac{1}{1-\frac{1}{m}}\|\nabla f(\mathbf{x}_{j+1})\| \\ &= \frac{m}{m-1}\|\nabla f(\mathbf{x}_{j+1})\|.\end{aligned}$$

It follows then that for any  $t \geq m$ , for any  $j \in [m]$ , we have

$$\begin{aligned}\|\nabla f(\mathbf{x}_{t-j})\| &\leq \left(\frac{m}{m-1}\right)^j \|\nabla f(\mathbf{x}_t)\| \\ &\leq \left(\frac{m}{m-1}\right)^m \|\nabla f(\mathbf{x}_t)\| \\ &\leq 4\|\nabla f(\mathbf{x}_t)\|,\end{aligned}$$

where the final inequality follows from the fact that the sequence  $\left(\frac{n}{n-1}\right)^n \leq 4$  for all  $n \geq 2$ .  $\square$

Next, we restate and prove Lemma 1, which shows that for any  $0 < c < 1$ , we can inductively guarantee that the gradient estimation bias  $\|\xi_t\|$  always satisfies  $\|\xi_t\| \leq c\|\nabla f(\mathbf{x}_t)\|$  for all  $t \geq m$ .

**Lemma 1.** *Suppose that Assumptions 1 and 2 hold. Suppose  $2 \leq m = \mathcal{O}(d)$ . Suppose we pick  $\tilde{\eta}$  such that it satisfies Condition 1. Then, for any  $0 < c < 1$ , by picking  $\eta = C\frac{1}{dC_dL}$  for some sufficiently small absolute constant  $C > 0$ , we can ensure that*

$$\|\xi_t\| = \|\mathbf{g}_t - \nabla f(\mathbf{x}_t)\| \leq c\|\nabla f(\mathbf{x}_t)\|$$

for any  $t \geq m$ .

*Proof.* We consider an inductive proof. Our inductive claim is as follows. Pick any  $t \geq m$ . suppose that the inductive assumption

$$\|\mathbf{x}_{j+1} - \mathbf{x}_j\| \leq 2\eta\|\nabla f(\mathbf{x}_j)\|$$

holds for all  $j < t$ . Then, for any  $0 < c < 1$ , by picking  $\eta = C\frac{1}{dC_dL}$  for some sufficiently small absolute constant  $C > 0$ , we will show that the inductive claim implies that

$$\begin{aligned}\|\xi_t\| &\leq c\|\nabla f(\mathbf{x}_t)\| \\ \implies \|\mathbf{x}_{t+1} - \mathbf{x}_t\| = \|\eta\mathbf{g}_t\| &\leq \eta(\|\nabla f(\mathbf{x}_t)\| + \|\xi_t\|) \leq 2\eta\|\nabla f(\mathbf{x}_t)\|,\end{aligned}$$

which inductively guarantees that  $\|\xi_{t'}\| \leq c\|\nabla f(\mathbf{x}_{t'})\|$  for all  $t' \geq t$ .

We first observe that our inductive assumption holds for the base case  $t = m$ , since by our assumption,

$$\|\mathbf{x}_{j+1} - \mathbf{x}_j\| \leq 2\eta\|\nabla f(\mathbf{x}_j)\|$$

holds for all  $j < m$ .

Let  $\eta_t$  denote the step-size at time  $t$ , which is  $\tilde{\eta}$  for any  $t < m$  and  $\eta$  after that. Observe that for any  $t \geq m$ ,<sup>5</sup>

$$\|\xi_t\| \leq \|\mathbf{g}_t - \nabla f(\hat{\mathbf{x}}_t)\| + \|\nabla f(\hat{\mathbf{x}}_t) - \nabla f(\mathbf{x}_t)\|$$

<sup>5</sup>For notational simplicity, our analysis below assumes that the first  $m$  iterations also utilizes the adaptive smoothing scheme. However, this is by no means necessary and we note that with some more tedious derivations, we can easily generalize the derivation to the case with no adaptive smoothing in the first  $m$  iterations and achieve the same bound.

$$\begin{aligned}
& \stackrel{(i)}{\leq} \|\mathbf{g}_t - \nabla f(\hat{\mathbf{x}}_t)\| + L\|\hat{\mathbf{x}}_t - \mathbf{x}_t\| \\
& \stackrel{(ii)}{\leq} \|\mathbf{g}_t - \nabla f(\hat{\mathbf{x}}_t)\| + \eta_{t-1}L\|\mathbf{g}_{t-1}\| \\
& \stackrel{(iii)}{\leq} C_d \frac{L}{2} \max_{i=1:m-1} \|\hat{\mathbf{x}}_{t-i} - \hat{\mathbf{x}}_t\| + \eta_{t-1}L\|\mathbf{g}_{t-1}\| \\
& = \frac{C_d L}{2} \max_{i=1:m-1} \left\| \sum_{j=1}^i (\hat{\mathbf{x}}_{t-j} - \hat{\mathbf{x}}_{t-j+1}) \right\| + \eta_{t-1}L\|\mathbf{g}_{t-1}\| \\
& = \frac{C_d L}{2} \max_{i=1:m-1} \left\| \sum_{j=1}^i (\mathbf{x}_{t-j} - \mathbf{x}_{t-j+1} + \delta_{t-j}\mathbf{u}_{t-j} - \delta_{t-j+1}\mathbf{u}_{t-j+1}) \right\| + \eta_{t-1}L\|\mathbf{g}_{t-1}\| \\
& = \frac{C_d L}{2} \max_{i=1:m-1} \left\| \sum_{j=1}^i (\mathbf{x}_{t-j} - \mathbf{x}_{t-j+1} + \eta_{t-j-1}\|\mathbf{g}_{t-j-1}\|\mathbf{u}_{t-j} - \eta_{t-j}\|\mathbf{g}_{t-j}\|\mathbf{u}_{t-j+1}) \right\| \\
& \quad + \eta_{t-1}L\|\mathbf{g}_{t-1}\| \\
& \stackrel{(iv)}{\leq} \frac{C_d L}{2} \max_{i=1:m-1} \left( \sum_{j=1}^i (\eta_{t-j}\|\mathbf{g}_{t-j}\| + \eta_{t-j-1}\|\mathbf{g}_{t-j-1}\| + \eta_{t-j}\|\mathbf{g}_{t-j}\|) \right) + \eta_{t-1}L\|\mathbf{g}_{t-1}\| \\
& \leq \frac{C_d L}{2} \max_{i=1:m-1} \left( \sum_{j=1}^i (2\eta_{t-j}\|\mathbf{g}_{t-j}\| + \eta_{t-j-1}\|\mathbf{g}_{t-j-1}\|) \right) + \eta_{t-1}L\|\mathbf{g}_{t-1}\| \\
& \stackrel{(v)}{\leq} \frac{C_d L}{2} \left( \sum_{j=1}^{m-1} (4\eta_{t-j}\|\mathbf{g}_{t-j}\| + \eta_{t-j-1}\|\mathbf{g}_{t-j-1}\|) \right) \\
& \leq \frac{C_d L}{2} \sum_{j=1}^m 4\eta_{t-j}\|\mathbf{g}_{t-j}\| \\
& \stackrel{(vi)}{=} \frac{C_d L}{2} \sum_{j=1}^m 4\|\mathbf{x}_{t-j+1} - \mathbf{x}_{t-j}\| \\
& \stackrel{(vii)}{\leq} 2C_d L \sum_{j=1}^m 2\eta\|\nabla f(\mathbf{x}_{t-j})\|,
\end{aligned}$$

where (i) holds by  $L$ -smoothness of  $f$ , (ii) holds by definition of  $\hat{\mathbf{x}}_t := \hat{\mathbf{x}}_t + \eta_{t-1}\|\mathbf{g}_{t-1}\|\mathbf{u}_t$  due to the adaptive selection of the smoothing radius  $\delta_t := \eta\|\mathbf{g}_{t-1}\|$  and the fact that each  $\mathbf{u}_t$  has unit norm, (iii) utilizes Assumption 2, (iv) again uses the fact that each  $\mathbf{u}_t$  has a unit norm, (v) holds by our assumption at the start of this subsection that  $C_d \geq 1$ , (vi) holds since  $\mathbf{x}_{t-j+1} = \mathbf{x}_{t-j} + \eta_{t-j}\mathbf{g}_{t-j}$ , and (vii) follows by our inductive assumption.

Now, utilizing our inductive assumption, we may also use Lemma 5 to find that for any  $j \in [m]$ ,  $\|\nabla f(\mathbf{x}_{t-j})\| \leq 4\|\nabla f(\mathbf{x}_t)\|$ . Thus, continuing from above, we find that

$$\begin{aligned}
\|\xi_t\| & \leq 2C_d L \sum_{j=1}^m 2\eta\|\nabla f(\mathbf{x}_{t-j})\| \\
& \leq 4C_d L \sum_{j=1}^m 4\eta\|\nabla f(\mathbf{x}_t)\|
\end{aligned}$$

$$\leq 16C_d L \eta \sum_{j=1}^m \|\nabla f(\mathbf{x}_t)\|.$$

Now, (recalling that  $m = \mathcal{O}(d)$ ), by picking  $\eta = \frac{C}{dC_d L}$  for a sufficiently small  $C > 0$ , we may conclude that

$$\begin{aligned} \|\xi_t\| &\leq c\|\nabla f(\mathbf{x}_t)\|, \\ \implies \|\mathbf{x}_{t+1} - \mathbf{x}_t\| &= \|\eta \mathbf{g}_t\| \leq \eta(\|\nabla f(\mathbf{x}_t)\| + \|\xi_t\|) \leq 2\eta\|\nabla f(\mathbf{x}_t)\|. \end{aligned}$$

Thus, by induction, since the base case of  $t = m$  holds, we can conclude that for all  $t \geq m$ , we have

$$\|\xi_t\| \leq c\|\nabla f(\mathbf{x}_t)\|,$$

as desired.  $\square$

We next restate and prove Theorem 1, which provides a convergence result for smooth nonconvex functions.

**Theorem 1.** *Suppose Assumptions 1 and 2 hold. Suppose  $2 \leq m = \mathcal{O}(d)$ . Suppose we pick  $\tilde{\eta}$  such that it satisfies Condition 1. Then, by picking  $\eta = C \frac{1}{dC_d L}$  for some sufficiently small absolute constant  $C > 0$ , for any  $T > m$ , the L-RESZO algorithm achieves*

$$\frac{1}{T} \sum_{t=m}^{T-1} \|\nabla f(\mathbf{x}_t)\|^2 \leq \mathcal{O}\left(\frac{dC_d L(f(\mathbf{x}_m) - f^*)}{T}\right).$$

*Proof.* By Lemma 2, we have that

$$f(\mathbf{x}_{t+1}) - f(\mathbf{x}_t) \leq -\frac{\eta}{8} \|\nabla f(\mathbf{x}_t)\|^2.$$

Summing this from  $t = m$  to  $t = T$  and plugging in our choice of  $\eta = \mathcal{O}\left(\frac{1}{dC_d L}\right)$ , we observe that

$$\begin{aligned} f(\mathbf{x}_T) - f(\mathbf{x}_m) &\leq -\mathcal{O}\left(\frac{1}{dC_d L} \sum_{t=m}^{T-1} \|\nabla f(\mathbf{x}_t)\|^2\right) \\ \implies \mathcal{O}\left(\frac{1}{dC_d L} \sum_{t=m}^{T-1} \|\nabla f(\mathbf{x}_t)\|^2\right) &\leq f(\mathbf{x}_m) - f(\mathbf{x}_T) \\ \implies \frac{1}{T} \sum_{t=m}^{T-1} \|\nabla f(\mathbf{x}_t)\|^2 &\leq \mathcal{O}\left(\frac{dC_d L(f(\mathbf{x}_m) - f^*)}{T}\right), \end{aligned}$$

where the final inequality uses the simple fact that  $f(\mathbf{x}_t) \geq f^*$ .  $\square$

We next restate and prove Theorem 2, which shows a linear convergence rate for smooth and strongly convex functions.

**Theorem 2.** *Suppose Assumptions 1 and 2 hold. Suppose  $2 \leq m = \mathcal{O}(d)$ . Suppose we pick  $\tilde{\eta}$  such that it satisfies Condition 1. Then, by picking  $\eta = C \frac{1}{dC_d L}$  for some sufficiently small absolute constant  $C > 0$ , for any  $T > m$ , the L-RESZO algorithm achieves*

$$f(\mathbf{x}_T) - f^* \leq \left(1 - \mathcal{O}\left(\frac{\mu}{C_d L d}\right)\right)^{T-m} (f(\mathbf{x}_m) - f^*).$$

*Proof.* Consider any positive integer  $t \geq m$ . By Lemma 2, we have that

$$\begin{aligned} f(\mathbf{x}_{t+1}) - f(\mathbf{x}_t) &\leq -\frac{\eta}{8} \|\nabla f(\mathbf{x}_t)\|^2 \\ &\leq -\frac{\eta\mu}{4} (f(\mathbf{x}_t) - f^*), \\ \implies f(\mathbf{x}_{t+1}) - f^* &\leq \left(1 - \frac{\eta\mu}{4}\right) (f(\mathbf{x}_t) - f^*), \end{aligned}$$

where the fourth inequality follows by  $\mu$ -strong convexity which ensures that  $\|\nabla f(\mathbf{x}_t)\|^2 \geq 2\mu(f(\mathbf{x}_t) - f^*)$ . Our desired result then follows.  $\square$

## B Empirical Study of $C_d$ in Assumption 2

We recall from Assumption 2 that the  $C_d$  term is defined as a positive ratio term such that

$$\|\mathbf{g}_t - \nabla f(\hat{\mathbf{x}}_t)\| \leq C_d \frac{L}{2} \max_{i=1:m-1} \|\hat{\mathbf{x}}_{t-i} - \hat{\mathbf{x}}_t\|.$$

In our empirical calculations below, for simplicity, we calculate this ratio  $C_d$  at the  $t$ -th iteration of the algorithm as

$$C_d(t) := \frac{\|\mathbf{g}_t - \nabla f(\hat{\mathbf{x}}_t)\|}{\frac{L}{2} \|\hat{\mathbf{x}}_{t-(m-1)} - \hat{\mathbf{x}}_t\|} \geq \frac{\|\mathbf{g}_t - \nabla f(\hat{\mathbf{x}}_t)\|}{\frac{L}{2} \max_{i=1:m-1} \|\hat{\mathbf{x}}_{t-i} - \hat{\mathbf{x}}_t\|},$$

and use our analytical knowledge of the ridge and logistic regression problems in (26) and (27) to compute the smoothness constant  $L$ .

### B.1 Ridge Regression

We experimented on the ridge regression problem in (26) for three values for the dimension  $d$ :  $d = 100, 400, 900$ . We computed the  $C_d$  ratio statistics for a trial of the algorithm for these three dimensions, and display this information in Table 3, which is based on the data from Figure 3; the corresponding convergence behavior is shown in Figure 4. We observe that the maximum  $C_d$  scales as around  $3\sqrt{d}$ , i.e.,  $\mathcal{O}(\sqrt{d})$ .

Table 3: Statistics of the  $C_d$  ratio across different dimensions  $d$  for the ridge regression problem (26).

Dimension $d$	Max	99th Percentile	Mean
100	25.1522	14.9690	3.9955
400	77.3924	53.6369	10.4881
900	104.1276	85.5617	18.3887

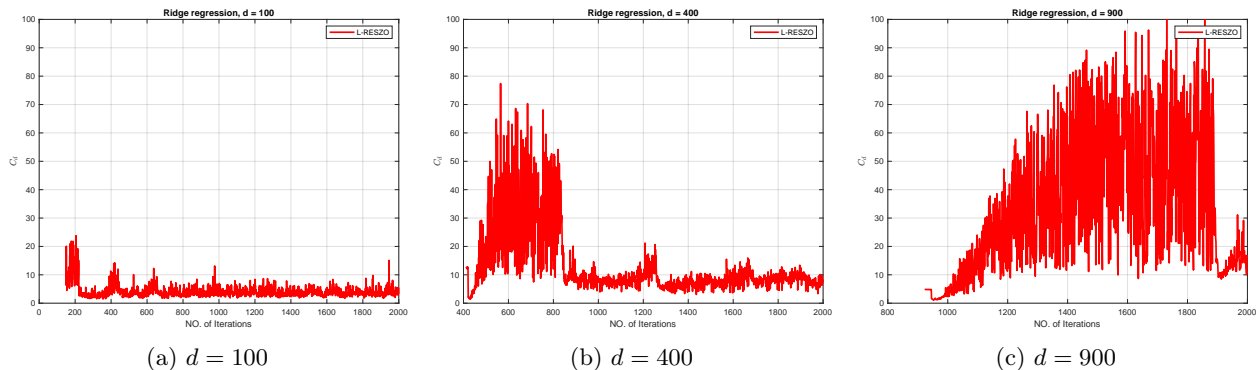


Figure 3: Empirical distribution of the ratio  $C_d$  for dimensions  $d = 100, 400, 900$  for ridge regression problem in (26). These plots are the sources from which the max/99-percentile/mean in Table 3 are computed.

### B.2 Logistic Regression

We experimented on the logistic regression problem (27) for three values for the dimension  $d$ :  $d = 100, 400, 900$ . We computed the  $C_d$  ratio statistics for a trial of the algorithm for these three

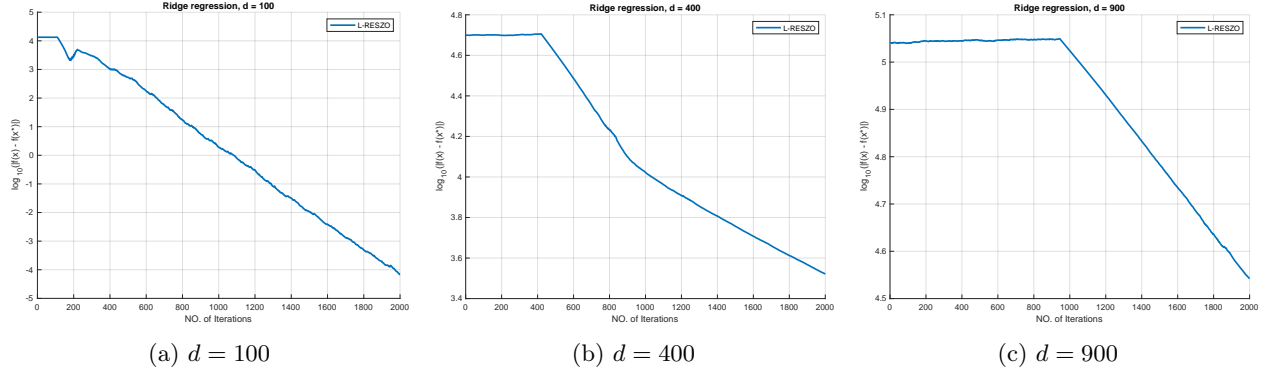


Figure 4: Convergence of L-RESZO on the ridge-regression problem in (26) for dimensions  $d = 100, 400, 900$ . The  $C_d$  ratios shown in Figure 3 are based on the algorithmic trajectories here.

dimensions, and display this information in Table 4, which is based on the data from Figure 5; the corresponding convergence behavior is shown in Figure 6. We observe that the maximum  $C_d$  scales as around  $2.5\sqrt{d}$ , i.e.,  $\mathcal{O}(\sqrt{d})$ .

Table 4: Statistics of the  $C_d$  ratio with different dimensions  $d$  for the logistic regression problem (27).

Dimension $d$	Max	99th Percentile	Mean
100	6.9935	2.8267	0.5665
400	47.2857	24.1032	3.7831
900	75.4320	64.0339	16.4693

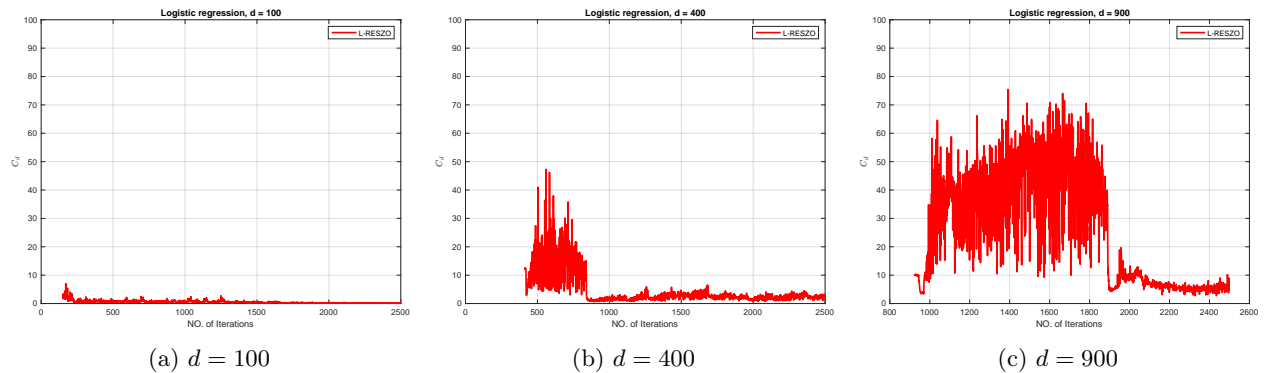


Figure 5: Empirical distribution of the ratio  $C_d$  for dimensions  $d = 100, 400, 900$  for logistic regression problem in (27). These plots are the sources from which the max/99-percentile/mean in Table 4 were computed.

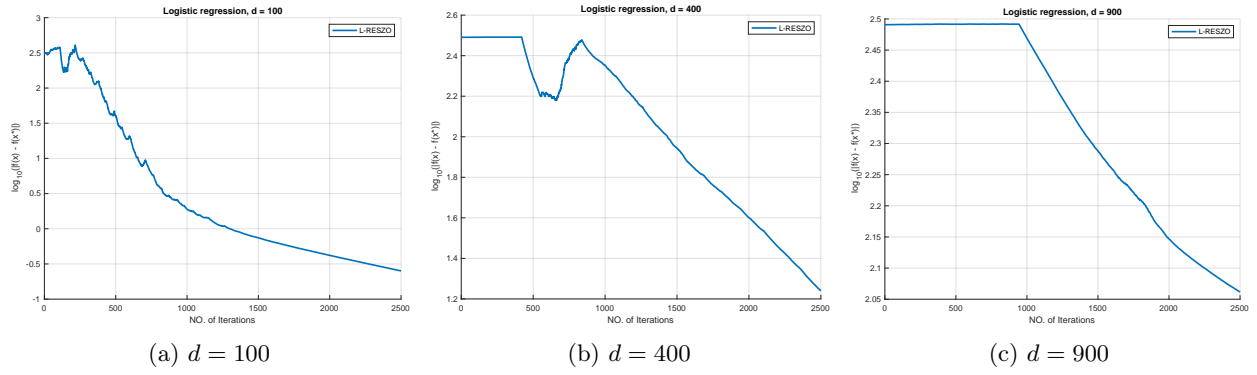


Figure 6: Convergence of L-RESZO on the logistic regression problem in (27) for dimensions  $d = 100, 400, 900$ . The  $C_d$  ratios shown in Figure 5 are based on the algorithmic trajectories here.